Journal of Molecular Liquids 354 (2022) 118895

Contents lists available at ScienceDirect

Journal of Molecular Liquids

journal homepage: www.elsevier.com/locate/molliq

Emerging optical and electrochemical biosensing approaches for detection of ciprofloxacin residues in food and environment samples: A comprehensive overview

Mohammad Javed Ansari [a], Dmitry Olegovich Bokov [b,c], Saade Abdalkareem Jasim [d,*], Mohammad Rudiansyah [e,*], Wanich Suksatan [f], Ghulam Yasin [g], Supat Chupradit [h], Ayad F. Alkaim [i], Yasser Fakri Mustafa [j], Dhuha Imad Tarek [k]

[a] Department of Pharmaceutics, College of Pharmacy, Prince Sattam Bin Abdulaziz University, Al-kharj, Saudi Arabia
[b] Institute of Pharmacy, Sechenov First Moscow State Medical University, 8 Trubetskaya St., bldg. 2, Moscow 119991, Russian Federation
[c] Laboratory of Food Chemistry, Federal Research Center of Nutrition, Biotechnology and Food Safety, 2/14 Ustyinsky pr., Moscow 109240, Russian Federation
[d] Al-maarif University College, Medical Laboratory Techniques Department, Al-anbar-Ramadi, Iraq
[e] Division of Nephrology & Hypertension, Department of Internal Medicine, Faculty of Medicine, Universitas Lambung Mangkurat/Ulin Hospital, Banjarmasin, Indonesia
[f] Faculty of Nursing, HRH Princess Chulabhorn College of Medical Science, Chulabhorn Royal Academy, Bangkok, Thailand
[g] Department of Botany, Bahauddin Zakariya University, Pakistan
[h] Department of Occupational Therapy, Faculty of Associated Medical Sciences, Chiang Mai University, Chiang Mai 50200, Thailand
[i] College of Science for Women, University of Babylon, Iraq
[j] Department of Pharmaceutical Chemistry, College of Pharmacy, University of Mosul, Mosul, Iraq
[k] Department of Optics, College of Health and Medical Technololgy, Al-Ayen University, Thi-Qar, Iraq

ARTICLE INFO

Article history:
Received 3 February 2022
Revised 3 March 2022
Accepted 5 March 2022
Available online 09 March 2022

Keywords:
Ciprofloxacin
Biosensor
Food safety
Antibiotics
Electrochemical sensor
Optical sensor

ABSTRACT

In today's world, despite the important role of antibiotics in human medicine, their accumulation in the human body through the food chain can pose serious health risks. The overuse of CFX (ciprofloxacin) as vital medicines to prevent and treat disease, improved feed conversion efficiency and preserve food has intensified in recent years. It is extremely urgent to progress a low-cost, rapid, and effective sensing technique for analyzing CFX residues in food and water resources. Till now, various analytical approaches have been proposed for CFX detection. (Bio)sensors have a hopeful viewpoint for rapid and on-site detection of CFX residues. This study focused on the recent progress and technical breakthroughs comprising electrochemical, optical nanoprobes for CFX detection in diverse matrices and proved how nanoprobes could enhance the performance of traditional sensing platforms. Well-known sensing platforms, working strategies, advantages and limitations of the research are also discussed, followed by prospects and challenges.

Contents

1. Introduction 2
2. Optical CFX nanoprobe 2

Abbreviations: CFX, Ciprofloxacin; MRLs, maximum residue limits; LC-MS, liquid chromatography/mass spectrometry; NMs, Nanomaterials; SPR, surface plasmon resonance; SERS, surface-enhanced Raman scattering; CdTe-QDs, cadmium telluride quantum dots; LOD, limit of detection; MMIP, magnetic molecularly imprinted polymers; Fe_3O_4, ferroferric oxide; MINs@PEGDA, molecularly imprinted nanoparticles@composite polyethyleneglycol diacrylate hydrogel; CDs, carbon dots; N-CDs, functionalized N-doped carbon dots; CNFs, carbon nanofibers; Tb^{+3}, terbium(III); LFA, lateral flow assay; LIL, laser interference lithography; AuNPs, gold nanoparticles; SWV, square wave voltammetry; CV, cyclic voltammetry; DPV, differential pulse voltammetry; β-CD, β-cyclodextrin; NiO-NPs, nickel oxide nanoparticles; CP, conducting polymers; PAR, poly alizarin red; MOFs, Metal-organic frameworks; ASV, anodic stripping voltammetry; GCE, glassy carbon electrode; COFs, covalent organic frameworks; FA, fluoroquinolone; PEC, (photoelectrochemical); C_3N_4/BiOCl, graphitic carbon nitride/BiOCl; g-C_3N_4, graphite-like carbon nitride.

* Corresponding authors at: Al-maarif University College, Medical Laboratory Techniques Department, Al-anbar-Ramadi, Iraq (S.A. Jasim). Division of Nephrology & Hypertension, Department of Internal Medicine, Faculty of Medicine, Universitas Lambung Mangkurat/Ulin Hospital, Banjarmasin, Indonesia (M. Rudiansyah).
E-mail addresses: saade.a.j@uoa.edu.iq (S. Abdalkareem Jasim), rudiansyah@ulm.ac.id (M. Rudiansyah).

https://doi.org/10.1016/j.molliq.2022.118895
0167-7322/

2.1. Fluorescence CFX nanoprobe . . . 2
2.2. Luminescence CFX nanoprobe . . . 4
2.3. Surface plasmon resonance CFX nanoprobe . . . 6
2.4. Surface-enhanced Raman scattering CFX nanoprobe . . . 7
3. Electrochemical CFX nanoprobe . . . 8
3.1. Voltammetric CFX nanoprobe . . . 8
3.2. Impedimetric CFX nanoprobe . . . 10
3.3. Potentiometric CFX nanoprobe . . . 12
3.4. Photoelectrochemical CFX nanoprobe . . . 12
4. Novel analysis devices . . . 14
5. Conclusions and future perspectives . . . 16
Declaration of Competing Interest . . . 16
Acknowledgements . . . 16
References . . . 16

1. Introduction

Antibiotics are secondary metabolites produced by microorganisms, as well as chemically synthesized or semi-synthesized chemical compounds [1]. Antibiotics are highly beneficial therapeutic agents which extensively utilized in both livestock and humans to prevent and treat various infectious diseases [2,3]. CFX is one of the clinical antibiotic drugs that can be used to cure numerous infectious diseases like urinary tract infections, gastrointestinal infections, lower respiratory tract infections pneumonia, skin and soft tissue infections owing to the low cross-resistance, quick and broad-spectrum bactericidal or bacteriostatic activity [4]. As a second-generation quinolone antibiotic, CFX is not entirely metabolized and persist in foodstuffs like eggs or milk or edible tissues. The production and usage of this antibiotic is high because of its low cost. Indeed, the misuse of CFX can increase the appearance of zoonotic CFX-resistant pathogens in animals along with some undesirable diseases and side effects like toxic and allergic reactions, intestinal flora disorders in humans through the food chain [5,6]. Owing to the adverse effects and increasing consumption of the quinolone residues, regulatory authorities, like the European Union, have determined MRLs (maximum residue limits) for FA (fluoroquinolones) in diverse animal-derived foods. The MRL for CFX residues has been set in some foodstuff by the Ministry of Agriculture of China and the European Commission at 100 ng mL^{-1} [7].

In this perspective, it is imminent to progress a series of on-site quick recognition approaches for rapid quantitative and screening of FA in food, environmental waters and bio-samples. Till now, various analytical methodologies were applied to determine CFX residues using microbiological tests and physical chemical methods. The chief utilized instrumental analysis is LC-MS (liquid chromatography/mass spectrometry), which offers high sensitivity and selectivity, however, requires expensive instrumentation, multiple-step in sample preparation, and proficient personnel to operate the equipment. In terms of microbiological tests, the main shortcomings are long incubation time and low specificity [8–10]. To overcome these issues, enormous efforts were focused on the progress of inexpensive, rapid, portable selective, and sensitive (bio)sensors for diagnosis and monitoring of CFX residues in an easily precisely and meticulously way in various matrices. As a compact analytical device, sensor are capable of highly quantitative/qualitative operation in sensing of various target biomolecules thanks to their rapid, cost-effective, reliable, real-time, and sensitive identification ability [11–14]. The specificity and sensitivity are two imperative properties of a biosensor [15–17]. The high sensitivity is typically influenced by the bioreceptor like synthetic MIP, DNA/RNA aptamer, antibody and enzyme, immobilization of biomolecule, and transduction technique, while the specificity has been achieved via an effective integration reaction between the transducer and biological constituents [18]. Application of appropriate bio-recognition element and NMs (nanomaterials) is vital strategies for enhancing the sensitivity and specificity of a sensor/biosensor. The amalgamation of nanotechnology in sensing scaffold can present a smart nanostructure, which in turn it could be applied as future analytical tools for CFX residues monitoring. It is well known that when NMs were utilized in sensing substrates, signal responses considerably enhanced as a result of target-bioreceptor interaction [19,20]. In view of their small size, optoelectronic, and high surface to volume ratio features, NMs were broadly engaged for the construction of clinical and field-deployable analytical devise for more efficient detection of analytes [21,22]. Besides, the incorporation of nano-engineered materials with sensors have significant effects on the effectiveness of sensing features in term of response time, reagent volumes, specificity, sensitivity, and cost of the device [23,24].

In recent years, a wide variety of sensing strategies have been developed to pursue practical applications for the quantification of CFX residues. As far as we know, there has not been a comprehensive study on sensor for the detection of CFX residues until now. Herein, in this overview, recent advances in isolation and determination techniques in the context of sensing have been discussed. Sensing strategies focusing on electrochemical nanoprobes and optical approaches (fluorescent, SPR (surface plasmon resonance), SERS (surface-enhanced Raman scattering) and luminescence. Meantime, the benefits and restrictions of different kinds of recognition strategies to consider the most rational and sensitive platform for the CFX residues were evaluated. Such signs of progress form the basis for a next generation point-of-care CFX analysis and other FA residues (Schematic 1).

2. Optical CFX nanoprobe

Over the last decade, the optical sensor has attracted considered attention as precious and significant analytical devices for activities like drug screening and sensing of widespread types of analytes such as biomarkers drugs, viruses, bacteria, cells and toxins due to several advantages such as high specificity, sensitivity, cost-effectiveness and small size sensing [25–27]. This type of simple and cheap sensor mainly is divided into five useful and practical groups including fluorescence, luminescence, SPR and SERS sensor [28]. Generally, an optical sensor is carried out by exploiting the interaction of the optical field with a bio-recognition element. This subsection is provided with a brief application of different types of optical methods for the detection of CFX.

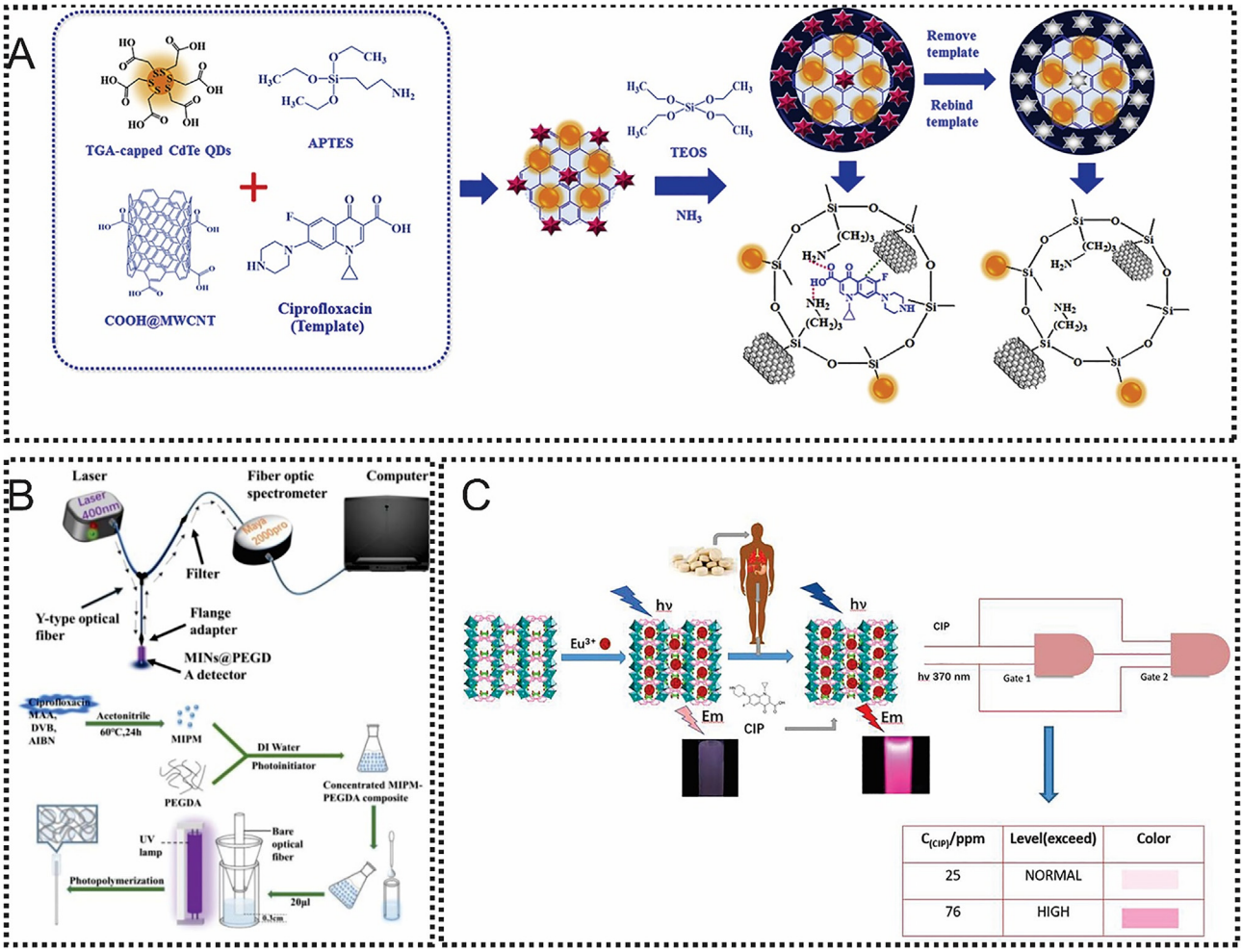

Fig. 1. **(A)** Illustration of CFX determination by fluorescence sensor. Reproduced with permission from Ref. [31]. Copyright Elsevier Science, 2018. **(B)** Schematic of fluorescence sensor based on MINs@PEGDA for CFX detection. Reproduced with permission from Ref. [37]. Copyright Elsevier Science, 2021. **(C)** Schematic of fluorescence-based sensor for detection of CFX. Reproduced with permission from Ref. [44]. Copyright Elsevier Science, 2020.

2.1. Fluorescence CFX nanoprobe

Fluorimeter is a popular analytical technique that uses ultraviolet light to excite the various NMs, oligonucleotides, and dyes for measuring the fluorescence signal during the return of these materials and biomaterials to their ground state due to the absorption of short wavelength radiation with higher energy [29,30]. Because of beneficial features including contactless detection, time-saving, and high sensitivity, this class of optical sensor was broadly used for CFX detection.

In 2018, Yuphintharakun et al. [31], developed a novel fluorescence optosensor based on implantation of COOH@MWCNT-MIP-QDs and CdTe-QDs (cadmium telluride quantum dots) in MIPs (molecularly imprinted polymers) for selective determination of CFX (Fig. 1A). MIPs are acted as artificial bioreceptor with several advantages including good thermal, mechanical and chemical stability to overcome the expensive and sophisticated fabrication procedures of common bioreceptors [32,33]. In this concept, the adsorption of CFX on the surface of the developed fluorescence probe was examined by fluorescence quenching. The measurement of fluorescence intensity in the designed sensor provided a sensitive and selective sensing platform of CFX with linear range and LOD (limit of detection) of 0.10–1.0 μg L^{-1} and 0.066 μg L^{-1}, respectively. Furthermore, recoveries of CFX in chicken and milk samples from 82.6% to 98.4%, indicating the acceptable accuracy of the reported platform. MIPs are a novel and preeminent termed as synthetic analogue to the natural, biological antibody-antigen platform. Incorporation of this type of non-biological receptor with various types of NMs such as carbon-based, silica-based and magnetic-based NMs have been offered high potential sensing tool for the efficient, low-cost and low detection limit of CFX [34,35]. In another sensing platform of CFX, Gao and colleagues [36], fabricated an innovative fluorescence sensor based on MMIP (magnetic molecularly imprinted polymers) consisting of CdTe-QDS and Fe_3O_4 (ferroferric oxide) NPs. The presence of Fe_3O_4 NPs in the core shell structure of MIP provided magnetically susceptible characteristics. Thereby, the reported optical sensor could efficient determination of CFX with LOD of and 130 ng mL^{-1}. With comparing of these two sensing substrates, it reveals that the sensitivity of the second nanoprobes has radically better owing to magnetic NMs in the MIP construction. The high potential of MIPs to recognize and bonding with CFX have caused the application of another type of MIPs in the structure of fluorescence sensor [37]. In this regard, MINs@PEGDA (molecularly imprinted nanoparticles@composite polyethyleneglycol diacrylate hydrogel) as a novel detector of CFX were integrated with optical fiber sensor by laser light source, an optical fiber spectrometer, a Y-type fiber, a computer and a flange adapter for providing rapid and highly selective fluorescence sensing platform for CFX determination (Fig. 1B).

Comparison of traditional MIPs with MIP-NPs dramatically demonstrated that MIP-NPs have higher sensitivity as a result of the interface ratio increasing, which induce more interaction between analyst and imprinted sites and cavities [38,39]. In the prepared sensor, the concentration of CFX has a direct relationship with fluorescence intensity (LOD = 6.86 μM). Despite enormous development in the application of the various types of synthesis MIP, Kojok et al. [40], proved that the sensitivity and selectivity of fluorescence immunosensor is second to none. For this purpose, a specific antibody was conjugated to CFX, creating a fluorescence probe on the CFX molecule. The intensity of fluorescence has a direct relationship with the concentration of CFX. The developed optical biodevice could able to detected CFX with a detection limit of 1 ppb. For the first time, Hu and colleagues [41], fabricated fluorescence-based aptasensor biosensor for CFX determination. In this study, $MoSe_2$ was exploited to coat CNT in the other to create scaffold for CFX capturing. This carbon-based nanomaterial played a critical role in establishing effective contacts and directing distribution of $MoSe_2$. Besides, the fluorescein-labeled aptamer was used to quenching of the designed NMs-based probe. The conjugation of aptamer with CFX caused the aptamer/G-quadruplex complex formation and the interaction between CNT-$MoSe_2$ complex and labeled aptamer was decreased. Under optimized experimental conditions, the reported aptamer based assay demonstrated a remarkable linear range and LOD of 0.63 to 80 nM and 0.63 nM, respectively. In addition, real-time identification of CFX resides in some milk samples was examined and 94.3% to 97.0 % as a recoveries were gained.

Over the last decade, several researchers have been attempted to exploitation various types of NMs including CDs (carbon dots), N-CDs (functionalized N-doped carbon dots), CNFs (carbon nanofibers), Eu^{3+}@1, Cu^{2+}–gold nanoclusters, Tb^{+3} (terbium(III)), silica nanoparticles, Al^{3+} and Cu^{+2}-gold in the signal on–off fluorescence system for developing a sensitive and selective optical analytical method of CFX [42–44]. For instance, Lu and co-workers [42] reported easy-to-use and ratiometric fluorescence assay based on the simple and efficient fluorescence probe for detection of CFX. CDs was coupled with riboflavin to form a dually emitting probe of CFX due to abundant functional groups including amino, hydroxyl and carboxyl groups. In the presence of CFX, the ratio of the relative fluorescence signal was linearly enhanced at 443 and 510 nm. Under optimum conditions, the developed fluorescence sensor could able to measured concentration of CFX in the range of 0.5–200 μM. The specificity, sensitivity and feasibility of designed method were evaluated. In this concept, remarkable features of CDs such as water solubility, excellent biocompatibility, low cost, hypotoxicity and unique optical properties have guaranteed the accurate of reported optical sensor (detection limit of 0.13 μM). Furthermore, under excitation at 370 nm, two emission peaks at the wavelengths of 443 nm and 510 nm have been appeared due to presence of riboflavin in the structure of probe. Therefore, carbon based NMs and riboflavin play an important role in the detection of this analyte. In another similar approach, Dang′s group used N-CDs as label-free sensing probe in the structure of fluorescence turn "on-off" detection system of CFX [43]. In the presence of CFX, the fluorescence intensity of bipyridine-Cu@N-CDs was quenched in the Cu^{2+} ions presence to measurement of CFX in the range of 0.05–50 μM. In the developed nanosensor, Cu^{2+} ions and bipyridine served as fluorescence quencher and linker between, respectively. Additionally, the tunable fluorescent properties N-CDs provided a unique sensing platform to quenched and recovered the fluorescence intensity. It should be noted that, the excellent recovery of 96–110% in real samples indicated promising of reported platform is detection of CFX.

Most recently, Wang et al. [45], used CNFs as another carbon-based fluorescence probe for *in-site* quantification of CFX. The system provided a great affinity towards to possess different functional groups on their surface of the CNFs. Furthermore, adsorption time of CFX on the CNFs is shorter than other type of carbon-based probes. The strong absorption of CFX on the surface of CNFs by – electron–donor–acceptor interaction, hydrophobic interaction and electrostatic interaction have caused difference in fluorescence intensity which measured by photometry mode of fluorescence spectrophotometer. Similarly, Wang and co-workers, [44] exploited Eu^{3+}@1 (as a highly fluorescent material) with interesting properties such as stability in water, porous channel and pH in-dependant for creating an ideal, and practical fluorescence probe (Fig. 1C). Thereby, capture of CFX by Eu^{3+}@1 has direct relationship with fluorescence signal intensity. It worth to noted that the assay provided satisfactory stability and alongside that acceptable sensitivity (LOD = 2.4 μg/mL or 2.4 ppm). The response time of target analyte in urine samples is less than 3 min, proving the potential of this fluorescence sensor for the determination of CFX in urine. Similarly, Chen and colleagues [46], designed a sensitive and selective fluorescence sensing platform based on Cu^{2+}-gold nanoclusters for detection of CFX. The reported fluorescence probe could efficiently capture this antibiotic owing to tunable fluorescence and reasonably strong in the NIR and visible region. In addition, to quench the strong fluorescence of the Au nanoclusters, Cu^{2+} has been used. In the presence of CFX, the fluorescence intensity of Cu^{2+}-Au complex was restored.

All things considered, the majority of developed fluorescence sensors based on artificial receptors and signal on–off system for the CFX have been exploited enormous types of carbon-based, silica-based and magnetic-based NMs for enhancing sensitivity and detectability of the system by improving the number of recognition regions at the polymer surface. The comparison of the various designed probes (summarized in Table 1) revealed that there is an immense shortage in the fabricating of various type of aptasensor, immunosensor, and also peptide-based probe in fluorescence sensor for detection of CFX.

In summary, fluorescent nanoprobes were extremely employed for determination of CFX in food. They also hold the excellent potential to be expanded in-field applications, especially with the progress of microfluidics systems and smartphone-based detectors. However, their quantification efficiency is continuously limited by the inherent photo-physical disadvantages of fluorophores like rapid photo-bleaching and instability in complex matrices. Besides, omitting signals in fluorescence sensors can be perturbed in harsh environmental situations. The emergence of new fluorescent nanomaterials would be mainly favorable for the construction of fluorescent probes with higher sensitivity, stability, accuracy, and reliability.

2.2. Luminescence CFX nanoprobe

Among different types of optical sensors, luminescence sensors have been carried out by light emission when an electron of a molecule is restored to the ground state after being excited for creating a powerful, popular and ideal analytical tool. The main advantages of luminescence-based biosensors are reproducibility, affordability and fast response. On the other hand, overcoming some limitations of these types of sensors including incompatibility with multiplexing and shortage of adequate sensitivity to different physicochemical variables are still challenge [47,48].

Over the last decade, several luminescence methods based on laser induced luminescence and lanthanides luminescence measurement have been reported for the estimation of CFX in biological fluids. In 2016, Singha et al. [49], introduced a simple and direct detection luminescence-based sensing platform for the determination of CFX in urine. As per this report, Tb^{+3} complex of DO3A (1,4,7,10-tetraazacyclododecane-1,4,7-triacetic acid) binds with

Table 1
Figures-of-merit of the reported optical-based sensors for efficiently quantification of CFX.

Detection method	Strategy	Sample type	Linear range	LOD	Ref.
Fluorescence-based sensors	A ratiometric fluorescent probe based on Al^{3+}-gold nanoclusters	Urine samples	–	1.4 nM	[149]
	COOH@MWCNT-MIP-QDs/MIPs optosensor	Chicken samples, milk samples and standard buffer	3.017–0.003 μM	1.991 μM	[31]
	Integration of MINs@PEGDA with optical fiber detector	Water samples and standard buffer	10–500 μM	6.86 μM	[37]
	Ratiometric fluorescence of CDs- riboflavin	Spiked water and human serum samples	0.5–200 μM	0.13 μM	[42]
	Fluorescence turn-on assay by Eu^{3+} functionalized Ga-MOF[a] Eu^{3+}@1	Urine samples and standard buffer	3.017–6.035 mM	0.007 mM	[44]
	Functionalized N-CDs in nanosensor structure	Spiked lake water and standard buffer	0.05–50 μM	0.4 nM	[43]
	Functionalized MIP with magnetic materials	Urine samples and standard buffer	–	0.392 μM	[36]
	A novel fluorescence probe based S-CDs[c]	Bovine raw milk	0.02–1.0 μM	6.7 nM	[150]
	A novel fluorescence probe based on carbon NMs	–	0.009–1.508 mM	0.301 μM	[45]
	MIPs@SiO_2-FITC	Aquaculture water	4.04–250 nM	4.04 nM	[151]
	EU-PS@MIBA as novel fluorescence probe based MIPs	Fish samples	0.001–0.301 nM	0.277 nM	[152]
	Microchip capillary	Milk supply	0.19 mM	–	[153]
	A tunable fluorescence probe based on Cu^{2+}–gold nanocluster	Urine samples	0.001–0.150 nM	9.053 nM	[46]
	Ratiometric fluorescence of CDs/silicon dots-CFX	Real biomedical samples	0.01–150 μM	2.0 nM	[154]
	LCPNP[d] probe	Biological samples	1.0 and 40 μM	780 nM	[155]
	Fluorescent siderophore pyoverdin	–	0–5 μM	7.13 μM	[156]
	Ratiometric fluorescence of Silicon nanoparticles-CFX	Food samples	0.211–132.4 μM	89 nM	[157]
	Surface decoration of cadmium-sulfide QDs with 3-mercaptopropionic acid as novel fluorescence probe	Pharmaceutical preparation and human serum samples	0.13–150.0 μM	0.04 μM	[158]
	A novel fluorescence probe based on Tb^{3+} and coordination polymer nanoparticles	Tablets and biological fluids	60 nM to 14 μM	60 nM	[159]
Fluorescence-based biosensors	Specific antibodies	Milk and human serum samples	–	0.003 μM	[40]
	Unique aptasensor based on aptamer/CNT-$MoSe_2$	Milk and human serum samples	0.001 to 0.241 μM	0.001 μM	[41]
	Tb^{3+}-DO3A as luminescence probe	Raw urine sample	0.003–0.150 mM	0.009 μM	[49]
Luminescence-based sensors	Microchip capillary	Spiked water samples	0.181–0.031 μM	0.009 μM	[52]
	Ag NPs-Eu^{3+}-CFX	Pharmaceutical and biological samples	0.06×10^{-7} to 0.03×10^{-5} M	0.057×10^{-8} M	[53]
	MINs on the sensing zone of SPR chip	Aqueous solution and synthetic wastewater	–	0.021 μM	[61]
SPR-based sensors	MIPs on the sensing zone of Gold SPR chip	Standard buffer	10 pM to 100 nM	~0.241 pM	[62]
	MIPs on the sensing zone of bimetallic chip	Water	–	0.1 pM	[160]
SERS-based biosensor	Immuno-nanoprobes on the test line of LFA	Buffer solutions and milk samples	–	0.001 nM	[65]
	SERS-LIL system based on anometric metallic patterns	Water samples	0–452 μM	3.018 μM	[71]
	Au–Ag bimetallic NPs as SERS active substrate	Water and chicken wings samples	–	8×10^{-8} and 2×10^{-7} M	[69]
SERS-based sensor	A novel SERS substrate based on Fe_3O_4 NPs@MIP dispersed on a silver solution	Water and serum samples	–	10^{-9} M	[68]
	Au NPs as stable and repeatable SERS substrate	Fish	0.001–0.03 mM	5.734 mM	[132]
	A novel SERS substrate based on Fe_3O_4/GO/Ag	–	10^{-6} to 10^{-9} M	Low down to 10^{-9} M	[161]
	Ag-TiO2 SERS strategy	Actual water samples	–	7.08×10^{-11} M	[137]

[b]Cadmium sulphide.
[a] Metal organic framework.
[c] Sulfur-doped carbon dots.
[d] Lanthanide coordination polymer nanoparticle.

CFX and emits characteristic terbium luminescence at 542 nm. The developed sensor could detect CFX without interference from the fluorescence components of the urine sample matrix and alongside that the sensitivity and linear range of the reported analytical device are acceptable (LOD = three parts per billion and linear range = 1 $\mu g \cdot mL^{-1}$ to 50 $\mu g \cdot mL^{-1}$). Furthermore, it does not require sample preparation steps and specialized fluorimeter. Recently, microchip capillary electrophoresis has become a development trend in real-time antibiotics detection because of its benefits like little sample size, low-cost, reduced analysis time to tens of seconds, infinitesimal waste amount and the probability of entirety combination of sample preparation [50,51]. Detectors are a key component in microchip capillary-based systems. An efficient combination of this type of sensing platform with the separation capillary and a detector is requisite for the ideal recognition of isolated targets. For creating a highly selective detection of antibiotics using capillary electrophoresis, the capillary was combined with a luminescence detector. For instance, Sierra-Rodero and co-workers, [52] fabricated a novel luminescence sensor based on Tb^{+3}-FQs chelates for efficient determination of CFX. For this purpose, the laser-induced of modification sensing zone of microchip capillary electrophoresis with Tb^{+3}-FQs-CFX was measured at wavelengths of 337/545 nm. The linear range and detection limit of the proposed platform are 10.6–60.0 ng mL^{-1} and 3.2 ng mL^{-1}, respectively. In addition, the ability of this sensing method for simultaneous detection of enrofloxacin, flumequine and CFX in less than 4 min is admirable.

Ag NPs have newly attracted considered attention in lanthanide luminescence systems as surface enhancers. The compatibility of mixing AgNPs with numerous matrixes such as dendrimers, poly-

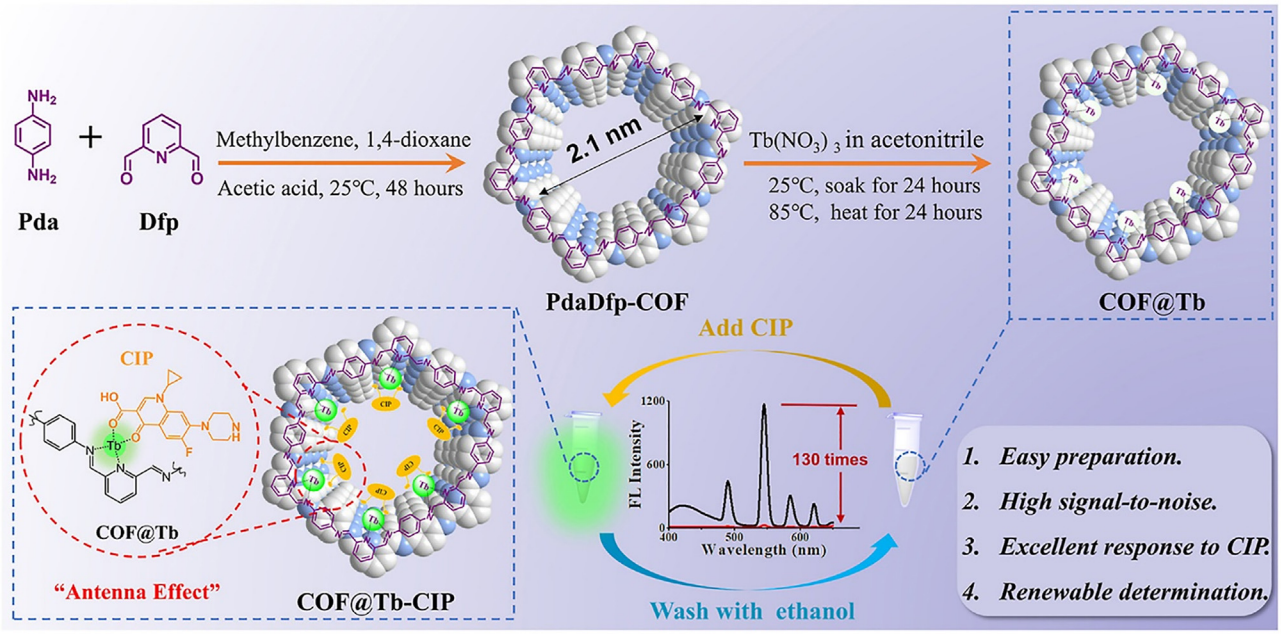

Fig. 2. Representation of the luminescence sensor for detection of CFX in based on COFs@Tb^{3+} as luminescence probe. Reproduced with permission from Ref. [54]. Copyright Elsevier Science, 2021.

mers, graphene, silicate network, and metal oxides improved sensing performance with high stability. The sensitivity and stability of the probes can be affected by the dispersion and prevention of the AgNPs aggregation in the matrices or network. These nanomaterials could intensify the fluorescence of lanthanide complexes. For example, Kamruzzaman and colleagues [53], reported metal NPs-enhanced fluorescence of their Eu^{3+}-CFX complex for amplifying and improving their luminescence. Lanthanides luminescence measurement system could able to measure all the photoluminescence spectra to detect CFX with LOD of 19×10^{-11} g mL^{-1}. Most recently, COFs (covalent organic frameworks) are a class of crystalline porous polymeric NMs with extremely ordered configurations and permanent porosity were suggested for fabrication of various nanoprobes. For example, Ren et al. [54], established a new luminescence-sensor using COFs due to superior thermal and solvent stability (Fig. 2). The conjugation of Tb^{3+} with new imine-linked COFs by the Schiff base reaction between 2,6-Diformylpyridine and P-phenylenediamine have provided a superb capacity to quantify CFX with a LOD of 3.01 nM. This designed luminescence sensor based on COFs may open the new windows for using porous organic materials in sensing of CFX.

All things considered, there is a huge shortage of luminescence-based sensors for CFX determination. Besides, various types of bioreceptors such as aptamer, antibody, enzyme and DNA can play a consequential role in the development of selective and sensitive luminescence systems.

2.3. Surface plasmon resonance CFX nanoprobe

SPR sensors as another prominent optical sensing technique, is thought to be favorable for perceiving the interaction between biomolecules and offering real time monitoring of binding events between various targets. In such a sensor, conjugation CFX along with different types of probes on the Au interface can change the refractive index at the chip surface that rely on the CFX mass and the starting angle of the resonance (incident) [55–57]. Several advantages of this sensing method including label-free, real-time and direct detection have caused received considered attention for CFX detection. However, some drawbacks of SPR-based sensors including bulky in size, sensitivity to temperature, long calibration process and sensitivity to motion cannot introduce these types of optical sensors as an efficient sensing approach. In 2011, a portable SPR immunosensor for quantification of CFX in milk was reported by Fernandez et al. [58]. In this concept, the SPReeta Evaluation Kit SPR3 with three-channel gold chips have modified with mixed self-assembled monolayers and FA haptenized protein. Hence, the conjugation of FA with antibody led to SPR signal decreases due to a change in the refractive index. Variety advantages of developed optical bioassay including affordability, portability and usefulness have been introduced high-performance laboratory SPR instrument for on-site concentration analysis of CFX. Current progresses in different developing disciplines have permitted the fabricate of innovative receptors for SPR sensors. Recently, the exploit of receptors coupled with molecular imprinting technique and nanotechnology has enhanced SPR instruments, Since then, several researchers have been attempted to create sensing methods using the SPR method and utilized to the identification of CFX residues in foodstuff [59,60]. For instance, Sari and co-workers [61], fabricated an innovative SPR nanosensor based on MINs for rapid and accurate determination of CFX. Due to their unique properties, the SPR chip surface was decorated with MINs for efficient capture of this antibiotic in an aqueous solution by creating recognition molecules on the sensing zone. Thus, binding of CFX to the specific cavities of MINs caused shifts on the refractive index of SPR nanosensor. High selectivity, high sensitivity, low cost and easy-to-use of MINs could provide a unique optical sensing platform with a detection limit of 7.1 ppb. In addition, the recovery results in spiked samples for CFX varied from 87 ± 4.6%. Similarly, Luo and colleagues [62], established SPR-based sensor for detection of CFX through linking of MIPs (as recognition element of CFX) on the surface of SPR sensor chip by in situ photoinitiated polymerization (Fig. 3). During the detection experiment of this study, the comparison of SPR response of CFX on MIP and non-MIP sensor presented acceptable reusability and excellent sensitivity (0.08 μg L^{-1}) with linear range of 10 pM to 100 nM.

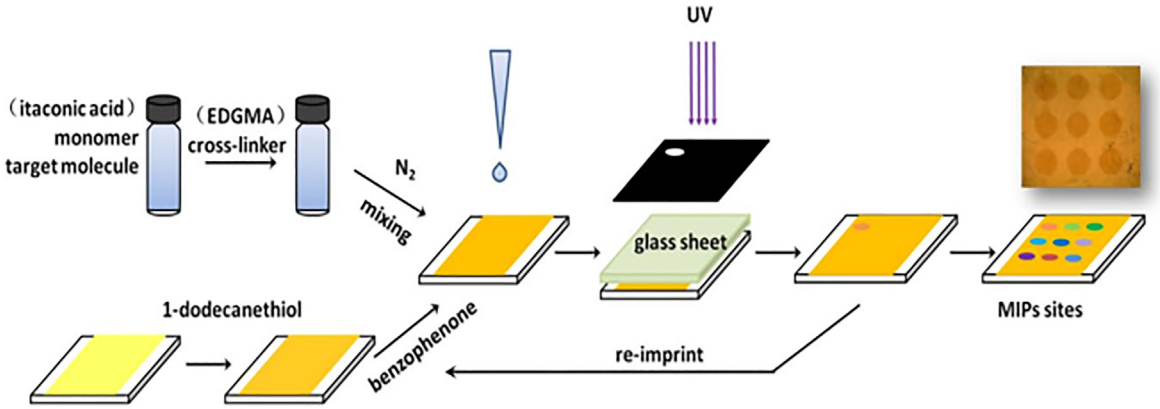

Fig. 3. Process of fabrication of SPR sensor based on MIPs for determination of CFX. Reproduced with permission from Ref. [62]. Copyright Elsevier Science, 2016.

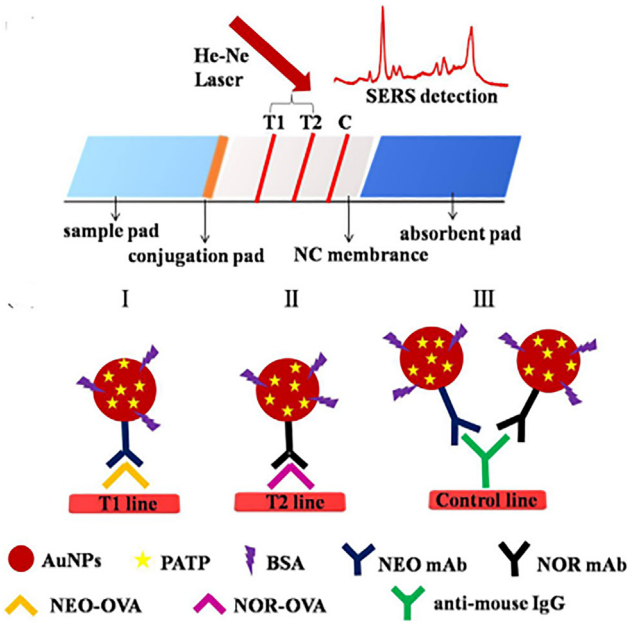

Fig. 4. SERS-based sensor for the detection of CFX. Reproduced with permission from Ref. [65]. Copyright springer Science, 2018.

The analytical performances of some SPR systems for CFX detection are summarized in Table 1.

Compared with other optical nanoprobes, SPR probes allow real-time monitoring of the CFX-probe binding with less reagent consumption. They are maybe the best effective instances of commercialized tools for CFX determination in food samples. Regardless of some portable SPR biosensors developing, however, most of them are still limited to the laboratory. Besides, their sensitivity and LOD for detection of CFX in food samples should be additionally enhanced. Another issue of SPR-based sensors is that MIP-decorated sensor chips demonstrate an unacceptable sensitivity due to small targets that can only induce small changes in the refractive index. However, the large size of CFX $C_{17}H_{18}FN_3O_3$ and the acceptable sensitivity of SPR-based sensors (Table 1) reveal that combined SPR with different types of nanoscale MIPs can provide a capable analytical technique of CFX under the WHO limit (100 ng. mL^{-1}).

2.4. Surface-enhanced Raman scattering CFX nanoprobe

SERS, because of facile execution, excellent sensitivity and specific vibrational fingerprint documentation was broadly used in diverse fields including food safety, biomarkers detection, homeland security, disease diagnostics and surface science. In this powerful analytical method, molecules absorbed on the SERS substrate surface increase the Raman scattering. On the contrary, the most formidable argument in favor of the limitation of these types of sensing platforms is that of SERS-based sensor disadvantages. To elaborate, the sensing zone degrades with time resulting in a reduction in signal. Furthermore, it needs intimate contact between CFX and the enhancing surface [63,64].

Recently, some researchers have combined LFA (lateral flow assay) and LIL (laser interference lithography) with the SERS technique for the development of low-cost and low sample consumption sensing approach based on SERS method for detection of CFX. For instance, Shi et al. [65], designed a selective and portable SERS-LFA immunosensor based on AuNPs (gold nanoparticles) for determination of CFX (Fig. 4). In this novel biodevice, two test regions of LFA strips were decorated with AuNPs coupled to the Raman active molecule 4-aminothiophenol was furtherly conjugated to the monoclonal antibody (as the SERS probes) against various antibiotics such as CFX. The concentration of CFX was measured via SERS of the PATP-coated AuNPs captured in the test line of an LFA. The detection limit of CFX in buffer solutions was 0.57×10^{-3} $ng.mL^{-1}$. In many contexts, simultaneous detection of multiple targets in food samples is indispensable for detection due to co-contamination caused by multiple harmful substances in a complex matrix often takes place in many cases.

The stability of SERS substrate with superior activity is essential for introducing a sensitive and selective sensing platform. During the past decade, great efforts have been made for different SERS-based sensors based on random metal complexes like colloid MNPs, dendritic metal constructions and magnetic nano-imprinted polymers for CFX detection [66–68]. For instance, Li and colleagues [69], successfully developed an active SERS platform in quick determination CFX by using heterostructured cube Au-Ag composites. For this purpose, Au-Ag bimetallic NPs mixed with the CFX and then dropped on an aluminum foil. Afterwards, the SERS spectra have measured based on the portable stabilized R. Laser explorer at 785 nm as an excitation wavelength. The unique pros of easy synthesis and control of AuNPs have led to the increased number of SERS sensors based on AuNPs. The LOD of the designed sensing platform for CFX in water and extracted from chicken wings were 8×10^{-8} and 2×10^{-7} M, respectively. In another similar SERS sensor, SERS combined with AgNPs den-

dritic that was arranged by a facile replacement response containing both Zn and $AgNO_3$ for CFX determination [70]. AgNPs with giant electric fields due to localized SPR have been widely used in SERS detection methods. Besides, there are several sharp edges along with nano-gaps in the structure of silver nanodendrites, so it was hoped that these nanostructures will give an important Raman enhancement element. Under optimized experimental conditions, 785-nm near-IR diode laser source (maximum at 300 mW), CFX was detected with a LOD of 20 ppb.

Although SERS sensors based on random substrates have several advantages such as easy-to-use in fabrication and high efficiency, these types of optical approaches suffer from matters associated with SERS intensity reproducibility and lack of spatial uniformity. Hong and co-workers [71], prepared a SERS-LIL sensor based on nanometric metallic patterns in solid supports for overcoming the limitation of random SERS substrates. In this work, the LIL technique permitted excellent substrate-tosubstrate geometric parameters variations. Hence, this method fabricated nanogratings in SERS detection of CFX in water. The limit of quantitation acquired in this designed sensor (~1 ppm) was acceptable. The remarkable benefits of these types of sensors including working very well with liquid and solid food have caused the development of SERS assays for quantitative and qualitative CFX in various types of real samples containing CFX. On the other hand, coordination between the SERS substrate, sample and laser is somewhat sophisticated. These types of sensitive sensors could detect CFX, in a LOD range of 7.08×10^{-11} M to 5.734 mM. Table 1 highlights the examples of the SERS-based (bio)sensing approaches for efficiently quantification of CFX. Various research revealed that SERS biosensors have been considered as hopeful instruments for the on-line monitoring of antibiotics residues. Even though the label-free one is susceptible to food matrix interference and poor sensitive, the label-based one shows brilliant sensitivity toward CFX residues through reporting the SERS spectra from the active labels. Even with this progress, it is still extremely difficult to use SERS probes as routine sensing devices for antibiotics in food. Future studies might emphasize the optimization of the measurement and construction conditions, development of high-performance SERS platform, and incorporation of the SERS method with cutting-edge sample pretreatment approaches like IMS, microfluidics, and so on, to simplify its widespread utilization in real foodstuffs.

3. Electrochemical CFX nanoprobe

Nowadays, electrochemical biosensors are the most shared and frequently utilized nanoprobes towards monitoring antibiotic residues detection because of their many advantages including time-effective procedure, higher sensitivity, straightforward construction procedure, requiring lower sample quantity, and the possibility of miniaturization (through combinations between charge (Q), current (I), potential (E), and time (t)) [72,73]. Indeed, an electrochemical nanoprobe is an incorporated device that offers quantitative/semi-quantitative analytical data based on a bio-recognition approach comprising an electrochemical transducer (e.g., a field-effect transistor or electrode) [74]. Moreover, electrochemical approaches could be coupled with diverse kinds of substrate particularly those for sample manipulation devices such as microfluidics chips, having an excellent advantage for antibiotics detection [75–78]. Till now, voltammetric techniques (SWV (square wave voltammetry), CV (cyclic voltammetry), DPV (differential pulse voltammetry), and stripping voltammetry) were significantly engaged for the efficient electrochemical detection of antibiotic CFX residues. However, electrochemical impedance spectroscopy and PEC (photoelectrochemical) have also achieved noticeable emphasis as a substitute choice for antibiotics detection [79]. A detailed outline of these methods has been made with respect to the sensor signal readout format, detection limit, and applications in Table 2. Besides, the principles behind each technique are drawn below.

Table 2
Representative various current electrochemical (Bio)sensors for CFX detection.

Transduction method	Sensing strategy	Type of real samples	Linear range	Limit of detection (LOD)	Ref
Differential pulse voltammetry (DPV) and cyclic voltammetry (CV)	Ag-β-CD nanocomposite developed via hydrothermal route	Runoff water and sheep serum	0.1–50 nM	0.028 nM	[85]
Voltammetric	Nanoprobe designed based on($(Ag–Au)_{mix}$NP) using β-cyclodextrin polymer	Aqueous medium	–	7.24 nM	[86]
Voltammetric	CFX nanoprobe developed based on NiONPs-GO-CTS: EPH/GCE	Biological fluid samples	0.040–0.97 μM	6.7 nM	[90]
Voltammetry and Impedance	PAR/EGR composite film was prepared	Pharmaceutical preparation and biological media	4×10^{-8} to 1.2×10^{-4} M	0.01 μM	[91]
Voltammetry and Impedance	rGO/PPR/GCE nanocomposite have been developed	serum sample	0.002–400 μM	2 nM	[93]
Voltammetry	CFX sensing based on PEI@Fe_3O_4@CNTs nanocomposite	Drug tablets, urine, and serum samples	0.03–70.0 μM	3.0 nM	[94]
Voltammetry	NH_2-UiO-66/RGO nanostructure used as working electrodes	Water	0.02–1 μM	6.67 nM	[97]
Voltammetry	3D Au-PAMAM/rGO nanocomposite	Local and pasteurized milk samples	1 mM to 1 nM	1 nM	[101]
Impedance	CNT-V_2O_5-CS/SPCE platform was developed	milk samples	0.5 to 64.0 nM	1.5 nM	[162]
Impedance	AuNPs-COFs has prepared via straightforward impregnation-reduction method	A variety of real samples	1.0×10^{-5} to 0.5 nM	2.34 fM	[117]
Impedance	poly(pyrrole − *N*-hydroxysuccinimide) film was electrogenerated onto electrode	–	1×10^{-12} to 1×10^{-6} g mL^{-1}	3.0 pM	[118]
Potentiometric	ultrasensitive wireless aptasensor using flexible freestanding graphene paper	–	0.03–20 pM and 20–150 pM	30.0 fM	[121]
PEC	CFX sensing has been performed based on g-CN/BiOCl substrate	real samples	0.5–1840 nM	0.2 nM	[134]
PEC	Ti_3C_2 nanostructures adorned on the graphitic carbon nitride	Real commercial sample	0.4–1000 nM	0.13 nM	[135]
PEC	Aptasensor was proposed based on $CuInS_2$/3DNG and Bi^{3+}/B-TiO_2/rGO	Milk samples	0.01–1000 ng mL^{-1}	3.3 pM	[99]

3.1. Voltammetric CFX nanoprobe

Voltammetric techniques, in which redox processes and redox active species are measured as a function of the voltage, or potential, applied to the electrode, are often used in electrochemical nanoprobes owing to their technical benefits over other electrochemical techniques [80]. The working electrode was dipped in a solution comprising electroactive types that could be evaluated via various potentials [81]. The capability to simply recognize the CFX residues through voltammetric peak potential makes it very selective and sensitive, which are discussed as follows:.

Recently, cyclodextrin associated metal NPs have been broadly applied for colorimetric sensing of cyanide, melamine, and metal ions [82,83]. Cyclodextrin based nanocomposite is also an appropriate scaffold for electrochemical sensing because of rapid electron transfer [84]. In this context, Gill et al. have recently proposed an electrochemical sensor based on CV and DPV techniques for recognition of CFX residues using Ag β-CD (silver nanoparticle modified β-cyclodextrin) nanocomposite as a host molecule [85]. In this work, owing to the host–guest interactions of β-CD, it was applied as an electro-catalytic electrode modifier to detect CFX in runoff water and sheep serum. Besides, the presence of Ag NPs in this nanocomposite offers the affluence of electron transport, which helps in the highly selective and sensitive determination of CFX. The suggested electrochemical nanoprobe offered a LOD at 0.028 nM with a linear range of 0.1–50 nM. In a similar study, George and coworkers developed a dual sensing substrate for detection of Mn (II) ion and CFX residues based on the synthesis of bimetallic NMs. β-CD mediated microwave technique was applied for the fabrication of bimetallic Ag-Au NPs in the aqueous medium. Indeed, under optimal conditions, the β-CD polymer delivers rational support for the proper CFX interaction with $(Ag\text{-}Au)_{mix}$NP and the induced aggregation makes it an appropriate electrochemical and optical probe for effectively sensing of CFX with a detection limit at 7.24 and 10.26 nM, respectively [86].

Metal oxide NPs were extensively used as an actual electrocatalyst for detection of different targets owing to their high organic capture ability, low cost and strong electrocatalytic activity [87]. NiO-NPs (nickel oxide nanoparticles) are low-cost and provide the same electrocatalytic characteristics of Pt, Pd or Ag of higher cost. Besides, NiO-NPs based electrodes have significant catalysis abilities for various targets, greater electrode surface area and rapid mass transport [88,89]. Although imperative achievements have been made on these nanomaterials, there are still some challenges that can be addressed, like toxicity, cost, and stability uncertainty in the electrode mechanism process. As well, for the synthesis of metal oxide nanomaterials, special and tedious conditions were needed, which can affect the stability, shape, and size of these materials and thereby reproducibility of the nanoprobe.

Santos and colleagues have been developed a voltammetric based sensor using a GCE (glassy carbon electrode) modified with NiO-NPs and graphene oxide nanostructures for simultaneous detection of CFX and paracetamol. In this study, the H_2SO_4/HNO_3 was used to oxidize GR into GO, then they modified GCE electrode with NiO-NPs and GO by electrodeposition. The established electrochemical probe displays a detection limit of 6.7 and 6.0 nM with linear ranges of 0.10–2.9 μM and 0.040–0.97 μM, respectively [90]. Currently, GO and rGO integrated with metallic nanomaterials have become a hot spot in the sensing substrate for further stimulating charge transfer. Indeed, the incorporation of various metal nanostructures with GO via covalent and non-covalent interaction can enhance the conductive and catalytic of GO performances. The hybrid materials are highly sensitive and selective toward targets in the measuring medium.

In recent years, modified electrodes were applied as nanoprobes for the voltammetric sensing of numerous electroactive biomolecules like dopamine, creatinine, cysteamine, folic acid and pyruvic acid. Modification of various electrodes to achieve high selectivity, compatibility, and sensitivity requires extensive research. The superb performance of these nanoprobes relies on different modifiers such as MNPs, CP (conducting polymers), and carbon materials. A recent study is now concentrating on nano-metal colloids and CP. In this regard, Zhang et al. developed a nanoprobe based on PAR (poly alizarin red)/graphene nanocomposite for voltammetric sensing of CFX residues. As a result of the hydroxyl and benzoquinone group, PAR can act as a receptor of protons, which simplifies the reaction balance and induces the charge transfer between the targets and the electrode [91]. PPR is another CP with several active quinone elements in the polymeric chain, offering two electrons to redox reaction. It has SO_3H and OH functional groups that cause it an ideal electron donor for charge transfer between analytes and electrode; so, PPR thin film affords an extremely promising position for CFX molecule to undergo oxidation [92]. Owing to the interaction of CFX-PPR, a higher peak current and also excellent selectivity can be obtained. In light of that, Chauhan and coworkers have designed a new nanoprobe for highly selective and rapid sensing of CFX based on the PPR electropolymerization afterwards rGO drop-casting. The electrochemical identification of CFX based on the electrocatalytic properties of rGO-PPR composite, in which PPR act as a redox element as a result of the —SO_3H and OH presence, although rGO offers a higher surface area and high conductance. The CFX electrooxidation has been performed via a secondary —NH group existing in CFX targets. In sum, the rGO-PPR-GCE platform shows a synergistic effect towards CFX with the lowest LOD (2 nM) and broader linear range (0.002–400 μM) [93]. Recently, an electrochemical sensor based on DPV was presented towards CFX using polyethyleneimine/fe_3O_4/carbon nanotubes substrate. As a result of the modest polymer conductivity together with high active sites of amine functional groups and excellent conductivity of CNTs, the suggested platform has a superb electrocatalytic influence on the CFX electro-oxidation. The presented technique exhibited a detection limit of 3.0 nM in the range of 0.03–70.0 μM [94]. These platforms demonstrated manifest benefits in both rapid sensing and simplicity. However, the described electrochemical nanoprobes operated by quantifying the electro-oxidation signal of CFX, are simply impeded by other organic molecules/structural analogs, and usually demanded high catalytic activity in electrode materials. Additionally, enhancements in detecting performance, for instance, reusability, sensitivity, selectivity, and acceptable stability, are still desirable for the low detection of CFX. On the other hand, direct application CNTs was restricted via poor dispersibility in polar solvents, which results in CNTs aggregation.

The CFX molecule can also be shaped as a stable composite with heavy metal cations like Cd^{2+} Pb^{2+}, and Cu^{2+} because the heterocyclic group, NH_2 group, and COOH group as electron-donating sites in CFX arranged via electron-deficient metal ions [95,96]. Based on the aforementioned issues, Fang and collaborator have designed a selective and sensitive electrochemical nanoprobe using Zr(IV)-based Metal-organic frameworks (MOFs) and RGO (NH_2-UiO-66/RGO) nanostructure toward CFX determination based on the CFX-Cu^{2+} complexation reaction [97]. As seen in Fig. 5A, through ASV (anodic stripping voltammetry), the Cu^{2+} reveals a high oxidization current on the modified electrode (NH_2-UiO-66/RGO), which declines in the CFX presence owing to the complex Cu^{2+}-CFX system. The Cu^{2+}peak current was engaged as the signal response for CFX identification, which in turn it displays much higher sensitivity in respect of the direct electrochemical oxidation. This nanoprobe can identify CFX at low trace levels (2.21 μg L^{-1}) and display excellent stability in the developed electrochemical platform.

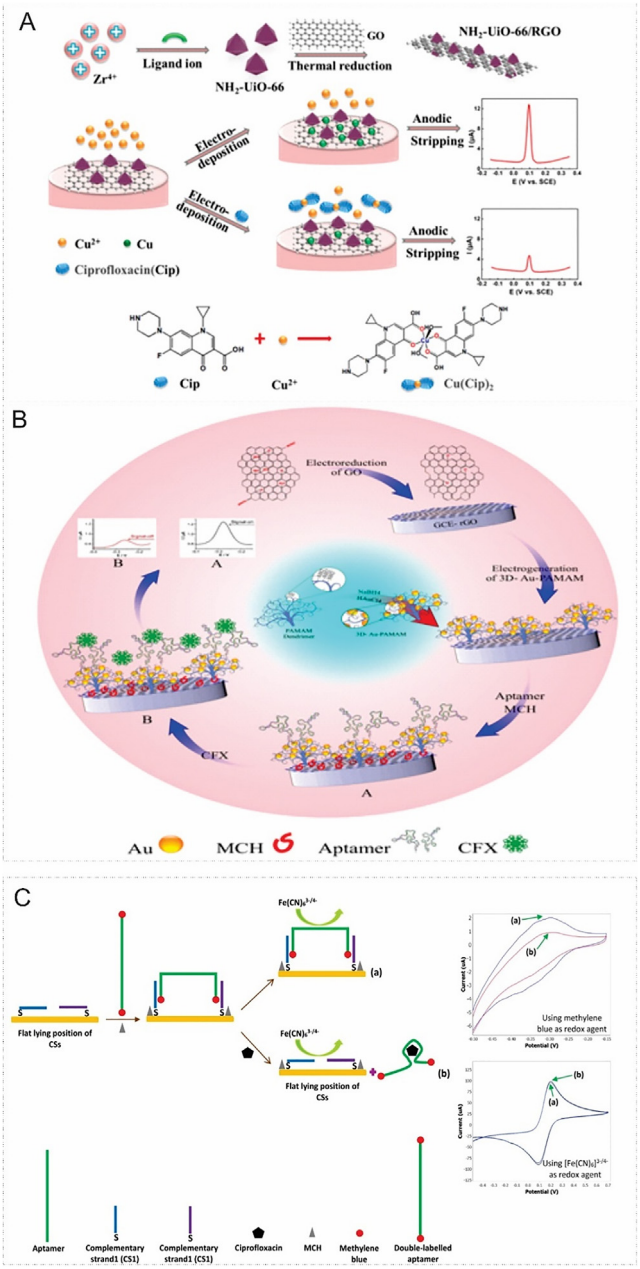

Fig. 5. **(A)** Diagrams of the NH_2-UiO-66/RGO synthesis process and the electrochemical CFX sensing. Reproduced with permission from Ref. [97]. Copyright American Chemical Society Science, 2019. **(B)** Schematic illustration of the rGO/3D Au-PAMAM aptasensor towards CFX detection. Reproduced with permission from Ref. [101]. Copyright Elsevier Science, 2021. **(C)** Drawing of the electrochemical nanoprobe for CFX identification using methylene blue (double-labelled aptamer). Reproduced with permission from Ref. [163]. Copyright Elsevier Science, 2021. (For interpretation of the references to color in this figure legend, the reader is referred to the web version of this article.)

Some voltammetric analyses were utilized specific aptamer rather than antibodies to determine antibiotic residues. Aptamers stand with their definite constructs which are designed using their sequences, can identify their ligands with high specificity and affinity. They are typically based on RNA or DNA and in comparison to antibodies, are more simple to work, less expensive and also may be utilized for identification of diversity of targets' ranging from ions to proteins. Biosensors wherein aptamers are used as a bio-recognition are termed aptasensors and they have been utilized for determination of CFX residues even more than immunosensor [98–100]. In a voltammetric aptasensor, Mahmoudpour et al. developed an easy-to use and sensitive approach using electrochemical single off toward CFX residues based on 3D Au-PAMAM/rGO nanocomposite. As shown in Fig. 5B, initially, the rGO has been formed on the GCE electrode by electroreduction of graphene oxide in PBS solution. Afterwards, as prepared 3D-Au-PAMAM via $HAuCl_4$chemical reduction in the PAMAM (poly amidoamine) existence as soft nanocontainers, and it was immobilized onto the modified rGO-GCE surface. Indeed, Au nanomaterial can be continuously dispersed via Amino-Au affinity in a polymer matrix, which shows smaller particle size and excellent stability in respect of the AuNPs prepared without a template. After specific CFX aptamer attachment, the 3D-Au-PAMAM/rGO probe ability can diagnose CFX residues in milk samples with a wide linear range of 1 mM to 1 nM and a low limit of quantification (LLOQ) of 1 nM [101].

In a study by Taghdisi Heidarian et al., an ultrasensitive electrochemical aptasensor (using voltammetric assay) has been established for evaluation of CFX residues based on MB-Apt-MB (double-labelled aptamer) and its CSs (complementary strands) [100]. The main advantage of the fabricated analytical probe is its ability to surpass the lying flat of CSs on the electrode interface which is the main challenge for DNA-electrochemical nanoprobe, particularly when the$[Fe(CN)_6]^{3-/4}$ was applied as a redox agent [102]. As depicted in Fig. 5C, in the absent of CFX, the double-labelled aptamer attaches on the interface of electrode by the assistance of CSs anchoring and since MBs are in the vicinity of the platform surface and a strong signal response could be realized. Nevertheless, in presence of CFX, the specific CFX aptamer is coupled to the analyte and the aptamer composition is modified, releasing the aptamer from its CSs, which is a proven phenomenon in the aptamer probes [103,104]. Overall, based on the proposed scaffold, the detection limit at100 pM with a dynamic range of 300 pM to 450 nM were obtained. Although various types of voltammetric sensors have been developed for CFX detection, the sensitivity of these types of electrochemical sensors to sample matrix effects can reduce the effectivity of voltammetric-based sensors for CFX determination.

3.2. Impedimetric CFX nanoprobe

In impedimetric techniques, the impedance of a device is detected in a wide range of frequencies. EIS (electrochemical impedance spectroscopy) is the most significant impedimetric analysis in electrochemical sensing in which the effective resistance of an electrical circuit depending on the sinusoidal alternating current potential with a small excitation amplitude is measured [105].

EIS is extremely sensitive to changes/interactions at a surface and herein, can be used to describe the numerous steps in building a biosensor that needs surface modification as well as calibration curve in which various molecule volumes are attached to the substrate surface [106,107]. The relevant parameters were generally obtained from EIS measurements by fitting the raw information to a device that models an equivalent circuit [108,109]. One of the most important benefits of EIS sensors over other electrochemical methods is their capability to implement in label-free mood, although to enhance sensitivity or selectivity, the labelling can be used [110,111]. Over recent years, EIS has played a significant role in the detection of different antibiotics because of their rapid detection times and high sensitivity. Herein, Hu et al. decorated the SPCE (screen-printed carbon electrodes) with some constituents containing chitosan polymer, biocompatible vanadium pentoxide (V_2O_5) NPs, and MWCNTs that serves as a stabilization substrate for the selective CFX aptamer (Fig. 6). Actually, the CFX aptamers can be anchored onto the modified electrodes through electrostatic interactions with cationic chitosan. The CFX binding

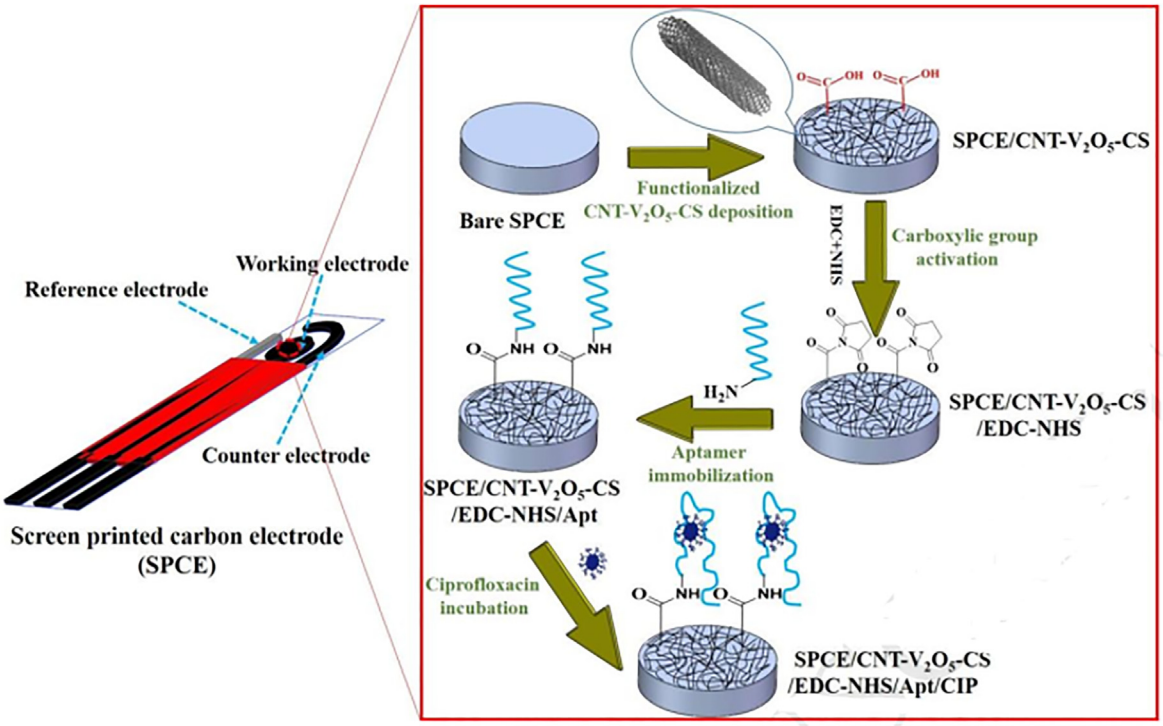

Fig. 6. Schematic representation of the CNT-V_2O_5-CS/SPCE electrode fabrication. Reproduced with permission from Ref. [112]. Copyright Elsevier Science, 2018.

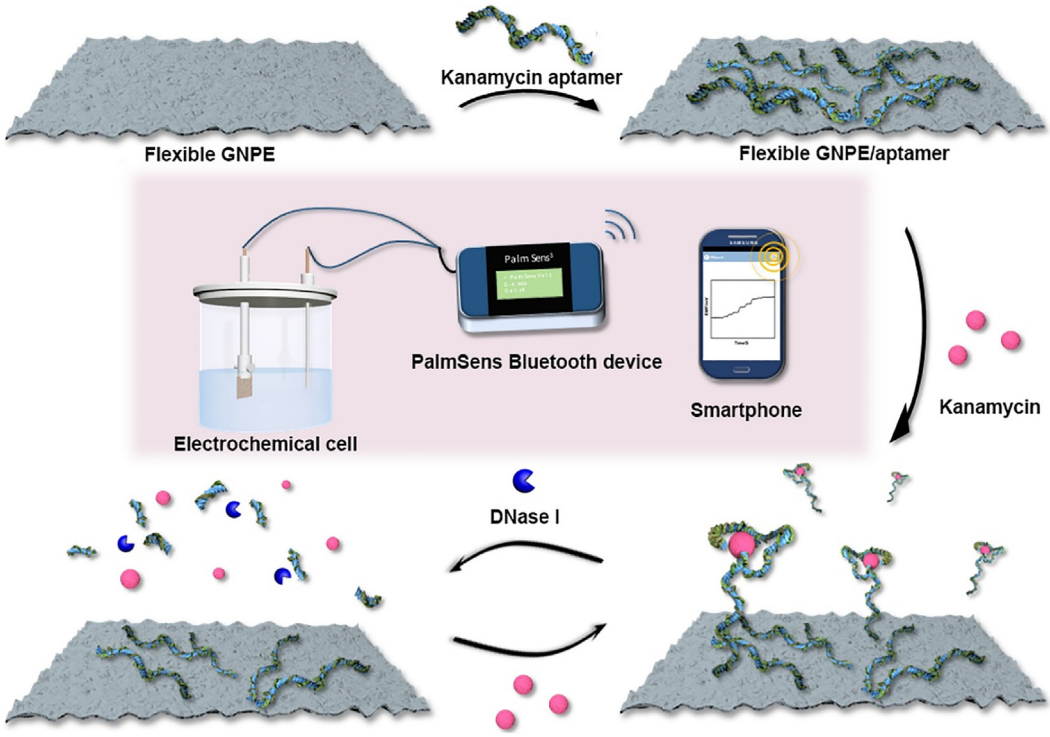

Fig. 7. Diagram of flexible freestanding GNP-based potentiometric enzymatic aptasensor. Reproduced with permission from ref. Copyright Elsevier Science, 2019.

can be improved the charge transfer resistance of the $Fe(CN)_6^{3-/4-}$ existing in the bulk phase that was shadowed via the EIS method. The suggested platform presented a low detection limit (0.5 nM), shows preferred selectivity even against the CFX structural analog -ENR and is permitted for the CFX detection in milk samples [112].

Until now, a variety of NMs were advanced to enhance the sensing signal like carbon nanomaterial, gold nanoparticle, MOFs, and so on. Nevertheless, the rational preparation of functional nanostructures to construct sensitive electrochemical aptasensors is of importance. As new and suitable porous ordered crystalline NMs, COFs were attracted immense attention in various fields, owning

to their high porosity, excellent stability, atomic level design, versatility and large channel [113]. COFs' properties bestow high-load capabilities of aptamer strands or biomolecules through various interaction forces, particularly π–π stacking and strong hydrogen bonds, to construct high-efficient COF-aptamer nanopores [114–116]. In this context, Zhu and collaborator have designed an AuNPs-COFs nanocomposite based on the straightforward impregnation-reduction technique for electrochemical impedimetric aptasensing toward CFX residues. In this study, AuNPs have been imbedded in porous nanostructures due to their biological compatibility, hypotoxicity, and superb conductivity to improve COFs deficiency. The EIS technique was successfully engaged for the quantitation of CFX in the range of 1.0×10^{-5}–0.5 nM with LOD of 2.34 fM [117].

Electrochemical impedimetric based on immunosensing assay form other types of bio-based CFX detection element. Here, the challenge arises from the definition of balance between the antibody-antigen (in such case CFX), antibody-electrode interface, and antibody-interfering.

interactions, which until now have been typically monitored using impedance spectroscopy. Fig. 7 presents an impedimetric CFX nanoprobe assembled on the GCE with N- hydroxysuccinimide, polypyrrole, which in turn is utilized as a linker coupled to the FA model target. Indeed, surface saturated with the CFX-antibody composite reveals excellent resistance to a charge transfer reaction of a redox probe existent in the bulk phase. This may be declined by the antibody desorption from the interface happening in the CFX existence. However, these nanoprobes were qualified only in the non-real situations and a lower detection limit at 3.0 pM was realized [118]. Substitute interface modification depends on the effective interactions of avidin-biotinylated antibodies [119]. This methodology provided a sensible substrate with the lower detection limit in the pM-nM ranges once susceptible to model CFX solutions. Amazingly, for the similar interface configuration, impedimetric CFX determination systems were quite diverse in the model real milk and environment samples. This discrepancy is described as the "construction of a dimeric calcium chelated form of the antibiotic" which limits the practical application of recommended substrate owing to inadequate understating of the assay mechanisms.

These types of electrochemical sensors have significant potential for use as simple and portable sensing devices. On the other hand, the main drawbacks of impedimetric-based sensors are the complexity of detection, susceptibility to non-specific binding and limitations to small molecule analysis. Besides, in order to fast performance of EIS, complicated voltage signal waveforms are required. Consequently, it can be challenging to detect CFX residues with EIS due to the exponential enhancement of the charge-transfer resistance through the polymer-protein layer to the underlying electrode surface and the high cost of complex instruments.

3.3. Potentiometric CFX nanoprobe

Potentiometric approaches, also known as controlled current techniques, in which the potential of an electrochemical cell have been measured in response to an applied current. The applied current is usually low amplitude. A benefit of controlled-current techniques is the capability to use low-cost measurement instrumentation relative to that required for controlled-potential approaches. Mainly, the progress of all-solid-state potentiometric nanoprobes have considerably.

improved the utilization of potentiometry in the analytical field, since they have tremendously facilitated the construction of sensing devices, enhanced the signal response, and more significantly, which could be coupled into miniaturized devices [120]. In light of that, Yao and coworkers established highly sensitive portable/wearable electronics using flexible freestanding.

graphene paper for monitoring of antibiotics residues. A schematic of the aptamer probes is presented in Fig. 7. the specific aptamers can attach to the graphene paper electrode interface by nuclease cleavage and π-π stacking is avoided as a result of hydrophobic forces between the graphene and aptamers. Once aptamers attach to analytes, it desorbs from the modified interface and has a tendency to isolate its negatively ionized phosphodiester elements. This charge variation induces a following alteration in the described potential values. Via un-immobilized nuclease in the sensing cell, the free aptamer strand is cleaved, hence releasing the antibiotics targets. The free molecules could hybridize by new aptamers on the surface of graphene paper electrode and recruit a new cleavage cycle, which causes an analyst recycling procedure. This causes an important signal enhancement and significantly increases detection sensitivity. The suggested platform allows determination linear ranges of 20–150 pM and 0.03–20 pM with an ultra-low detection limit of 30.0 fg mL^{-1} [121]. All in all, the most pivotal argument in favor of potentiometric sensors is that of the inundated number of benefits. The first advantage of these types of electrochemical biosensors is the selective measure of CFX in different environments. The second benefit of such a sensing approach is label-free detection of CFX. This, of course, comes with some downsides. Potentiometric sensors are sensitive to surrounding temperature.

3.4. Photoelectrochemical CFX nanoprobe

PEC sensing and biosensing are emerging diagnostic technique that has attracted much attention from researchers owing to the advantages of ultra-high accuracy, rapid response, simple operation, inexpensive instrument, and reduced background signal [122,123]. On the contrary, the main challenges and limitations of PEC sensors are biomolecule damage, high-energy light sources requirement for materials with large band gaps and PEC instability caused by photocorrosion. Compared with the optical technique, the PEC method is portable, simple to be miniaturized and inexpensive, giving it a promising prospect of real-time identification. In this examination, the electric signal is engaged as a recognition signal and the light is engaged as an excitation source, which in turn significantly declines the background signal. The photoactive nanomaterial under light irradiation can be excited to induce photo-generated electron-hole pairs, and then it is transferred to surface of the electrode, which offers photocurrent and realizes the photo-energy conversion to electrical energy [124,125].

Proper selection of NMs with superior PEC features is of importance in PEC measurements. Therefore, tremendous efforts were paid to explore and developing PEC NMs with high light harvesting, brilliant stability, and effective photoelectric conversion performance. Till now, various semiconductor materials were extremely examined as PEC materials like Bi_2MoO_6, BiOCl, $BiVO_4$, and so on [126,127]. BiOBr, as one of Bi based semiconductor NMs, can attract researchers' attention because of its charge transfer capability, efficient visible light absorption, and exceptional lamellar crystal building. BiOBr has four PbFCI (matlockite) layered crystal construction consisting of $[Bi_2O_2]^{2+}$ and two Br-ion layer building arranged alternately along the C axis, providing appropriate probability for the polarization of atomic orbital and atoms. This can improve the PEC performance by separating electrons and light-induced holes [128]. Nevertheless, the BiOBr band gap is around 2.64–2.91 eV, causing weak light absorption in visible regions and restricting possible presentation. The deposition of metal NPs into the semiconductor NMs can be a good choice. Thanks to the long carrier mean free path, small carrier effective mass, low carrier density, narrow band gap, and highly anisotropic

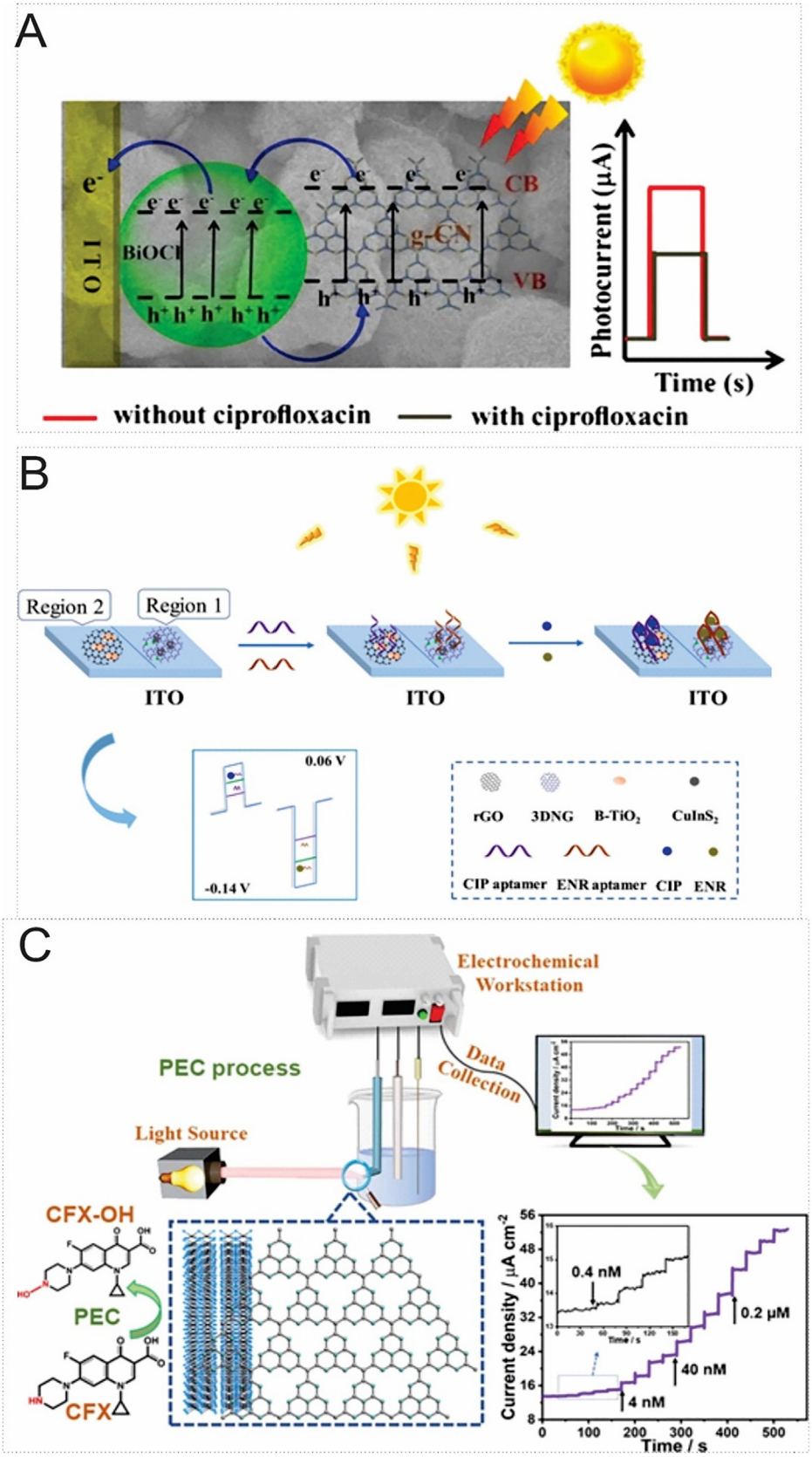

Fig. 8. **(A)** Representation of PEC sensor based on g-C_3N_4/BiOCl nanocomposite for CFX detection. Reproduced with permission from Ref. [134]. Copyright Elsevier Science, 2016. **(B)** Depiction of established PEC mechanism at g-C_3N_4-Ti_3C_2 nanocomposite for CFX identification. Reproduced with permission from Ref. [135]. Copyright Elsevier Science, 2021. **(C)** Procedure of the PEC aptasensor construction for the dual antibiotics sensing. Reproduced with permission from Ref. [99]. Copyright Elsevier Science, 2021.

Fermi surface, bismuth can improve the PEC feature. After BiOBr was doped with bismuth, the Bi/BiOBr composite offered flower-like configuration comprising various nanosheets [129]. The Bi/BiOBr photocurrent has been significantly enhanced 5-times to BiOBr. By means of Bi/BiOBr/ITO as a working electrode, CFX can be determined using the photocurrent change caused by the CFX addition because of the electron transfer inhibition.

Recently, integrating functional nanostructures are extensively used to improve the PEC performance in the monitoring of CFX residues. Most earlier described semiconductor NMs have consisted of metal sulfides, metal oxides and N-doped carbon NMs, comprising MOF, CdS, TiO_2, g-C_3N_4, and N-G quantum dots [130–133]. Herein, Xu and coworkers have developed a g-C_3N_4/BiOCl (graphitic carbon nitride/BiOCl) nanocomposite for a facile and sensitive PEC substrate to detection of CFX (Fig. 8A) [134]. The g-C_3N_4 (Graphite-like carbon nitride) has the band gap of ca. 2.7 eV, environmentally benignity, absorption of visible light along with photochemical and thermal stability owing to the p-conjugated construction and high amount of polymerization. Regardless of its advantages, shortcomings like small specific surface area, low conductivity, high exciton recombination rate and low absorption of visible light, still limit its practical applications. To increase its feasibility, they combined g-C_3N_4 with bismuth oxyhalides semiconductors for PEC sensing of CFX. A broad linear range of 0.5–1840 ng mL^{-1} with detection limit of 0.2 ng·mL^{-1} was produced by the suggested PEC biosensor.

In the other work, Yuan et al. [135] have designed a 2D/2D g-C_3N_4/Ti_3C_2 nanoprobe as a photosensitive nanomaterial via electrostatic self-assembly to realize highly selective and sensitive PEC determination of CFX (Fig. 8B). Indeed, the specific 2D configuration of Ti_3C_2 with a high amount of -O terminations advantages to create the heterojunction using Ti_3C_2 and other semiconductors via electrostatic adsorption, creating robust surface contact between semiconductors and Ti_3C_2, which in turn Ti_3C_2 can be worked as cocatalyts in the heterojunction [136,137]. Moreover, DFT (Density Functional Theory) calculation was demonstrated that the Fermi level of O-terminated Ti_3C_2 (0.58 V vs. NHE) is positive and higher than the conduction band of g-C_3N_4 (- 0.80 eV vs. RHE), signifying that Ti_3C_2 can efficiently capture photo-excited electrons from g-C_3N_4 and improve the electron/hole pairs separation. The CFX was measured in the linear range of 0.4–1 × 10^3 nM with the detection limit of 0.13 nM. Additionally, the proposed PEC probe has long-term stability, good selectivity and reproducibility.

Nowadays, owing to the separation of the detection signal (current) and excitation source (light), and the presentation of an aptamer as a biological recognition unit, PEC aptamer nanoprobes demonstrate a low cost, rapid signal response, higher selectivity, sensitivity, and affinity in comparison to classical electrochemical sensing methods [138,139]. PEC active material and aptamer strand are two independent fragments in the PEC aptamer probes in which the aptamer strand is associated with the substrate selectivity, while the identification sensitivity is more closely related to the PEC active materials. Actually, via subtle incorporation of the PEC sensing substrate and specific aptamer together, it is feasible yet popular to achieve quantitative/qualitative analysis of CFX. Most PEC platforms are quite restricted in their capability to multiplex detection of various target biomolecules. According to the literature, bias potential controlling technologies were used for the PEC sensing of sole analytes [140,141], however, this method is seldom utilized in PEC probes for the determination of multiple molecules. Indeed, multiplex sensing can be achieved via employing a diverse bias potential to inhibit interference between the photocurrent of NMs. In this context, a sensitive bias-potential-based PEC aptamer probe was designed and constructed for the simultaneous sensing of dual antibiotic residues, CFX and enrofloxacin, which often coexist in milk samples [99]. As seen in Fig. 8C, two nanocomposites with superb PEC performance have been advanced: $CuInS_2$/3DNG (3-D nitrogen doped graphene-loaded copper indium disulfide) and Bi^{3+}/B-TiO_2/rGO (Bi^{3+}-doped black anatase titania NPs coupled with reduced graphene oxide). By application of altered bias potentials to the two suggested composite nearby one electrode interface, the anodic and cathodic currents generated by Bi^{3+}/B-TiO_2/rGO and $CuInS_2$/3DNH can be discriminated. Then, CFX and ENR aptamers have been respectively immobilized onto the modified ITO interface to construct a PEC-aptamer based sensor for the highly sensing of CFX and ENR. Under optimal conditions, the suggested nanoprobes have the advantages of satisfying linear ranges of CFX (0.01–1000 ng mL^{-1}) and ENR (0.01–10000 ng mL^{-1}), and detection limit of as low as 3.3 pg mL^{-1} to CFX and ENR (S/N = 3).

The main importance of all the PEC based nanoprobes for antibiotics detection is practical application. Conventional PEC based probes typically could not meet the need for simultaneous determination of targets because of their limited sensing surface on the chip, which in turn restricted their practical employments. Emerging split-kind of PEC based sensor and incorporating PEC biosensing with microfluidics, arrays, and chips would contribute to high-throughput and automation. Furthermore, point of care detection can be realized by portable PEC substrates mixing PEC sensing with miniaturized signalling tools and hand-held devices.

4. Novel analysis devices

Conventional sensing devices and bio-devices are suffering from non-portability. Over the last decade portable, small, wireless, integrated, and flexible analytical devices have quickly emerged such as CCD (charge-coupled device)-based platform [142], smartphone-based sensor [143], microfluidic devices [144] and smart packaging [145] for providing easy operation, low-cost, portability and alongside that point of care detection of CFX. Hence, we review innovative approaches currently under development. Several analytical platforms have been established for CFX sensing based on the interaction of CFX with aptamer, antibody, enzyme and MIP. In 2018, Kao et al. [146], fabricated a portable biosensor using 16 individual bioluminescent wells of a whole-cell sensor array chip with a windowless linear CCD for CFX determination. They provided live bacterial cells as the sensing entities that are the most noticeable assay organisms for detecting CFX. In the presence of CFX, a CCD-based platform was exploited for monitoring of luminescent responses of the bioreporter bacteria (Fig. 9A). The designed biodevice indicated excellent response time (20 and 80 min) and LOD (64 ng/mL for egg yolk, 8 ng/mL for chicken essence, egg white and milk).

In another biosensor, Liu and co-workers [147], integration of QD microsphere immunochromatographic strip with a smartphone for point of care detection of CFX (Fig. 9B). This sensing zone has attracted considered attention as one of the emerging and rapid sensing substrates for point-of-care CFX testing. Furthermore, the integration of this bio-device with an intelligent smartphone have caused creation of automatically and conveniently florescence reader by smartphone camera (P30 pro, Huawei, China). Besides, smartphone have ability to upload the testing results via the wireless mobile network. The designed probe (QD monoclonal antibody) conjugated with CFX and were unable to be caught by the CFX-BSA interaction dispersed along the T lines. As result, the intensity of fluorescence was decreased. The reported portable bio-device could quantitative CFX with a low detection limit and a wide linear detection range. It should be noted, smartphones could not have the capability for optical detection and these types of wireless bio-devices can use for data interpretation collection and alongside that transmission.

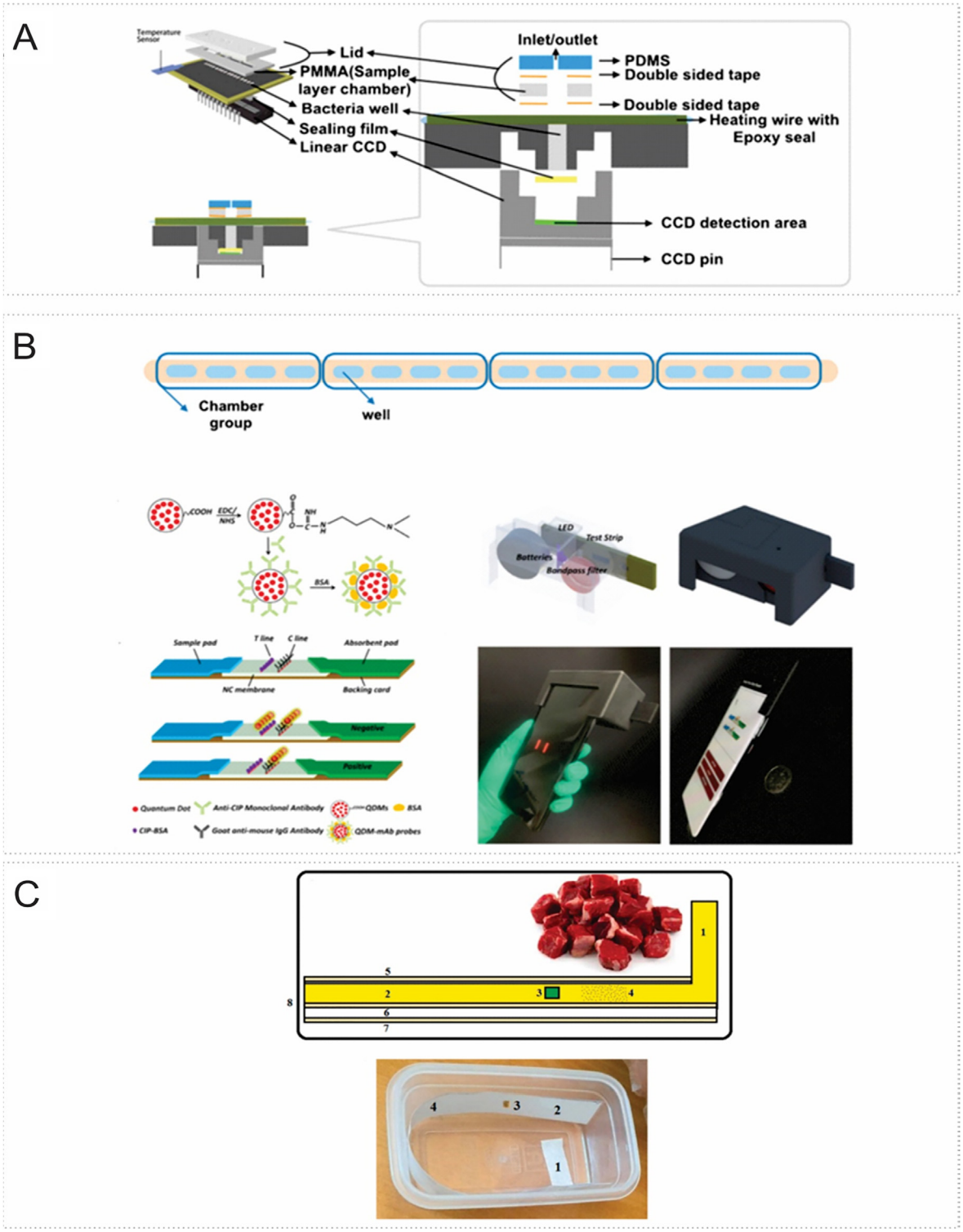

Fig. 9. **(A)** Components schematic of CCD-based platform for detection of CFX. Reproduced with permission from Ref. [146]. Copyright springer Science, 2018. **(B)** Schematic illustration of the CFX determination based on integration of smartphone and immunochromatographic strip. Reproduced with permission from Ref. [147]. Copyright Elsevier Science, 2021. **(C)** Illustration of the smart packaging designed for CFX detection. Reproduced with permission from Ref. [148]. Copyright Elsevier Science, 2021.

Smart packaging as one of the novel and low-cost types of sensors, have provided worthwhile info about spoilage, storage conditions, and maybe CFX residues. For instance, Tafti and colleagues [148], developed a simple and efficient smart packaging based on immune-chromatography to demonstrated CFX residues in beef meat. For this purpose, the surface of a cellulose tape (25 cm*1 cm) was modified with an anti-CFX antibody conjugated with AuNPs to the prepared first active surface. Then, a paper having anti-CFX antibodies was held as the second active interface. CFX was conjugated with antibody-AuNPs, resulting in this complex bonding with the antibody on the second active surface. The fabricated construction can fix on the inner wall of the food packaging. This sandwich assay on the sensing surface has caused tangible color change based on CFX concentration. It should be noted, they

used the first and second adsorbent surface for absorption of bloody water on and collecting excess water, respectively. The possible CFX amount in all meat samples has been tested via ELISA.

It is important to point out that, although amalgamation of sensing devices with small-size portable technologies like microfluidic tools and smartphone based substrates have provided promising technologies to enable rapid, outside-the-lab detection, there is some shortage in the utilization of these types of novel sensing approaches for determination of CFX.

5. Conclusions and future perspectives

A wide range of electrochemical and optical sensing approaches has been studied to overcome the problems associated with conventional detection of CFX resides due to the high potential of CFX in the safety and quality of foods and water. Generally, conventional techniques were employed as a powerful sensing platform; however, these require high-cost, preparation of the specimen, and trained technicians. Herein, promotion of sensitive and selective sensing devices towards quantitative detection of CFX in diverse matrices are highly desirable. Thereinto, optical and electrochemical sensors as useful diagnostic tools make it urgent, rapid analysis and as an answer for the mentioned issues. In this review, we have revealed a snapshot of the newest improvements in the nano and bio-sensors field and a summary of approaches for signals based on the utilization of various types of bio-receptors. Excitingly, with the incorporation of polymer nanomaterial chemistry and optical physics into the biosensor progress, the sensitivity was significantly enhanced in these recent years. Despite, NMs being used efficiently for signal enhancement, they can also act as perfect carriers for the attachment of various bioreceptors and direct detection of CFX. Although a few optical biosensors have been developed for determination of CFX, there is an enormous lack in the application of different types of bioreceptors including aptamer, antibody and enzyme for sensitive and selective CFX detection. In the developed electrochemical sensor for detection of CFX, there is a massive shortage in the use of portable devices for point of care detection. The insufficient number of portable devices signifies that construction of CFX nanoprobes with commercialization potential is still highly desirable. Investigation in the field of antibiotics platforms, particularly CFX probes, is still immature in comparison with other sensing grounds. In terms of nanostructures based substrates, various technical hurdles like appropriate linking between the bio-recognition unite and NPs, the non-uniform NPs influence on the performance of the sensor, biocompatibility of nanostructures with the bio-recognition unites, and interactions within CFX molecule should be intended. Besides, many existing sensing approaches have been limited to the laboratory scale and are not yet extended to the end user. Indeed, their selectivity and sensitivity can be impressed by real sample media, such as interfering constituents (e.g., carbohydrates, vitamins, proteins, and lipids), pH, viscosity, and ionic strength.

In the future, biosensing approaches in combination with novel bio-receptors and nanomaterials remain attractive with various exciting possibilities. More and more attention is focused on the application of advanced biosensing techniques with automated and portable miniaturized devices like smartphones and microfluidic devices to provide nanoprobes with portable, automated, integrated, and practical characteristics. Additionally, with the progress of information technology, biosensors in combination with big data analytics might have enormous potential to effectively predict and monitor CFX resides in the whole food supply chain for food control and safety. In summary, with the rational design of smart nanostructures based on flexible/biocompatible probes as well as the progress of lab-on-a-chip and 3D printed devices, significant commercial nanoprobes indirect analysis of various antibiotics in complex environments can come true in the near future.

Declaration of interest.

The authors declare that they have no known competing financial interests or personal relationships that could have appeared to influence the work reported in this paper.

Declaration of Competing Interest

The authors declare that they have no known competing financial interests or personal relationships that could have appeared to influence the work reported in this paper.

Acknowledgements

The authors would like to acknowledge the supports from the Department of Pharmaceutics, College of Pharmacy, Prince Sattam Bin Abdulaziz University,Al-kharj, Saudi Arabia.

References

[1] J. Lyu, L. Yang, L. Zhang, B. Ye, L. Wang, Environ. Pollut. 266 (2020) 115147.
[2] A. Sharma, G. Istamboulie, A. Hayat, G. Catanante, S. Bhand, J.L. Marty, Sens. Actuat., B 245 (2017) 507.
[3] Y. Ben, C. Fu, M. Hu, L. Liu, M.H. Wong, C. Zheng, Environ. Res. 169 (2019) 483.
[4] T. Thai, B.H. Salisbury, P.M. Zito, StatPearls [Internet], 2020.
[5] T. Chen, L. Zhong, Z. Yang, Z. Mou, L. Liu, Y. Wang, J. Sun, W. Lei, Chem. Res. Chin. Univ. 36 (2020) 1083.
[6] K. Rudnicki, K. Sipa, M. Brycht, P. Borgul, S. Skrzypek, L. Poltorak, TrAC, Trends Anal. Chem. 128 (2020) 115907.
[7] M. Tumini, O. Nagel, M.P. Molina, R. Althaus, Int. Dairy J. 64 (2017) 9.
[8] W. Jiang, N.V. Beloglazova, Z. Wang, H. Jiang, K. Wen, S. De Saeger, P. Luo, Y. Wu, J. Shen, Biosens. Bioelectron. 66 (2015) 124.
[9] H. Gao, G. Cheng, H. Wang, T. Chen, C. Xu, H. Lv, H. Zhang, R. Hou, Y. Wang, D. Peng, Microchem. J. 160 (2021) 105683.
[10] T. Liang, L.M. Leung, B. Opene, W.E. Fondrie, Y.I. Lee, C.E. Chandler, S.H. Yoon, Y. Doi, R.K. Ernst, D.R. Goodlett, Anal. Chem. 91 (2018) 1286.
[11] M. Mahmoudpour, S. Ding, Z. Lyu, G. Ebrahimi, D. Du, J. Ezzati Nazhad Dolatabadi, M. Torbati, Y. Lin, Nano Today 39 (2021) 101177.
[12] M. Mahmoudpour, J. Ezzati Nazhad Dolatabadi, M. Torbati, A. Pirpour Tazehkand, A. Homayouni-Rad, M. de la Guardia, Biosens. Bioelectron. 143 (2019) 111603.
[13] H. Karimi-Maleh, M.L. Yola, N. Atar, Y. Orooji, F. Karimi, P.S. Kumar, J. Rouhi, M. Baghayeri, J. Colloid Interface Sci. 592 (2021) 174.
[14] H. Karimi-Maleh, M. Alizadeh, Y. Orooji, F. Karimi, M. Baghayeri, J. Rouhi, S. Tajik, H. Beitollahi, S. Agarwal, V.K. Gupta, Ind. Eng. Chem. Res. 60 (2021) 816.
[15] H. Karimi-Maleh, A. Khataee, F. Karimi, M. Baghayeri, L. Fu, J. Rouhi, C. Karaman, O. Karaman, R. Boukherroub, Chemosphere (2021) 132928.
[16] H. Karimi-Maleh, F. Karimi, L. Fu, A.L. Sanati, M. Alizadeh, C. Karaman, Y. Orooji, J. Hazard. Mater. 423 (2022) 127058.
[17] H. Karimi-Maleh, Y. Orooji, F. Karimi, M. Alizadeh, M. Baghayeri, J. Rouhi, S. Tajik, H. Beitollahi, S. Agarwal, V.K. Gupta, Biosens. Bioelectron. 184 (2021) 113252.
[18] M. Majdinasab, M. Yaqub, A. Rahim, G. Catanante, A. Hayat, J.L. Marty, Sensors 17 (2017) 1947.
[19] Y. Chen, X. Li, G. Cai, M. Li, D. Tang, Electrochem. Commun. 125 (2021) 106987.
[20] Z. Yu, G. Cai, X. Liu, D. Tang, Anal. Chem. 93 (2021) 2916.
[21] J. Shu, D. Tang, Anal. Chem. 92 (2019) 363.
[22] Q. Zhou, D. Tang, TrAC, Trends Anal. Chem. 124 (2020) 115814.
[23] G. Maduraiveeran, M. Sasidharan, V. Ganesan, Biosens. Bioelectron. 103 (2018) 113.
[24] L. Lan, Y. Yao, J. Ping, Y. Ying, Biosens. Bioelectron. 91 (2017) 504.
[25] S. Lv, Y. Tang, K. Zhang, D. Tang, Anal. Chem. 90 (2018) 14121.
[26] Z. Qiu, J. Shu, D. Tang, Anal. Chem. 89 (2017) 5152.
[27] R. Ren, G. Cai, Z. Yu, Y. Zeng, D. Tang, Anal. Chem. 90 (2018) 11099.
[28] S.M. Borisov, O.S. Wolfbeis, Chem. Rev. 108 (2008) 423.
[29] S.M. Sundaresan, S. Fothergill, T.A. Tabish, M. Ryan, F. Xie, Appl. Phys. Rev. 8 (2021) 041311.

[30] M. Zandi, S. Zandi, R. Mohammadi, P. Hosseini, S. Teymouri, S. Soltani, A. Rasouli, Biotechnol. Appl. Biochem. (2021).
[31] N. Yuphintharakun, P. Nurerk, K. Chullasat, P. Kanatharana, F. Davis, D. Sooksawat, O. Bunkoed, Spectrochim. Acta Part A Mol. Biomol. Spectrosc. 201 (2018) 382.
[32] J.J. BelBruno, Chem. Rev. 119 (2018) 94.
[33] M.C. Carneiro, A. Sousa-Castillo, M.A. Correa-Duarte, M.G.F. Sales, Biosens. Bioelectron. 146 (2019) 111761.
[34] J. Ji, Z. Zhou, X. Zhao, J. Sun, X. Sun, Biosens. Bioelectron. 66 (2015) 590.
[35] X. Zhou, X. Gao, F. Song, C. Wang, F. Chu, S. Wu, Appl. Surf. Sci. 423 (2017) 810.
[36] B. Gao, X.P. He, Y. Jiang, J.T. Wei, H. Suo, C. Zhao, J. Sep. Sci. 37 (2014) 3753.
[37] Q.-D. Huang, C.-H. Lv, X.-L. Yuan, M. He, J.-P. Lai, H. Sun, Sens. Actuat., B 328 (2021) 129000.
[38] M. Mahmoudpour, M. Torbati, M.-M. Mousavi, M. de la Guardia, J. Ezzati Nazhad Dolatabadi, TrAC, Trends Anal. Chem. 129 (2020) 115943.
[39] H.K. Kordasht, M. Pazhuhi, P. Pashazadeh-Panahi, M. Hasanzadeh, N. Shadjou, TrAC, Trends Anal. Chem. 124 (2020) 115778.
[40] H. El Kojok, N. El Darra, M. Khalil, A. Capo, A. Pennacchio, M. Staiano, A. Camarca, S. D'Auria, A. Varriale, Sci. Rep. 10 (2020) 1.
[41] X. Hu, P. Wei, G. Catanante, Z. Li, J.L. Marty, Z. Zhu, Microchim. Acta 186 (2019) 1.
[42] C. Lu, G. Liu, Z. Yang, Y. Wang, H. Rao, W. Zhang, B. Jing, X. Wang, Microchim. Acta 187 (2020) 1.
[43] V.D. Dang, A.B. Ganganboina, R.-A. Doong, ACS Appl. Mater. Interf. 12 (2020) 32247.
[44] B. Wang, B. Yan, Talanta 208 (2020) 120438.
[45] X. Li, W. Wang, J. Dou, J. Gao, S. Chen, X. Quan, H. Zhao, J. Water Process Eng. 9 (2016) e14.
[46] Z. Chen, S. Qian, J. Chen, J. Cai, S. Wu, Z. Cai, Talanta 94 (2012) 240.
[47] Z. Yu, H. Gong, Y. Li, J. Xu, J. Zhang, Y. Zeng, X. Liu, D. Tang, Anal. Chem. 93 (2021) 13389.
[48] Z. Yin, L. Zhu, Z. Lv, M. Li, D. Tang, Talanta 233 (2021) 122563.
[49] S. Singha, K.H. Ahn, Sensors 16 (2016) 2065.
[50] Y. Zhang, X. Hu, Q. Wang, Talanta 232 (2021) 122410.
[51] R. Bosma, University of Guelph, 2019.
[52] M. Sierra-Rodero, J.M. Fernández-Romero, A. Gómez-Hens, Microchim. Acta 181 (2014) 1897.
[53] M. Kamruzzaman, A.-M. Alam, K.M. Kim, S.H. Lee, Y.S. Suh, Y.H. Kim, S.H. Kim, S.H. Oh, J. Nanosci. Nanotechnol. 12 (2012) 6125.
[54] Q. Ren, P. Yang, J. Liu, Y. Chen, S. Ouyang, Y. Zeng, P. Zhao, J. Tao, Anal. Chim. Acta 1188 (2021) 339191.
[55] H.K. Kordasht, M. Hasanzadeh, Talanta (2020) 121436.
[56] H.K. Kordasht, M. Hasanzadeh, F. Seidi, P.M. Alizadeh, Trac-Trends Anal. Chem. 140 (2021).
[57] M. Mahmoudpour, J. Ezzati Nazhad Dolatabadi, M. Torbati, A. Homayouni-Rad, Biosens. Bioelectron. 127 (2019) 72.
[58] F. Fernandez, D.G. Pinacho, F. Sanchez-Baeza, M.P. Marco, J. Agric. Food. Chem. 59 (2011) 5036.
[59] E.A. Türkoğlu, Applications of Nanomaterials in Agriculture, Food Science, and Medicine, IGI Global, 2021, p. 1–28.
[60] M. Khan, Crit. Rev. Anal. Chem. (2020) 1.
[61] E. Sari, R. Üzek, M. Duman, A. Denizli, J. Biomater. Sci. Polym. Ed. 29 (2018) 1302.
[62] Q. Luo, N. Yu, C. Shi, X. Wang, J. Wu, Talanta 161 (2016) 797.
[63] M. Muhammad, Q. Huang, Talanta 227 (2021) 122188.
[64] C. Lin, L. Li, J. Feng, Y. Zhang, X. Lin, H. Guo, R. Li, Microchim. Acta 189 (2022) 1.
[65] Q. Shi, J. Huang, Y. Sun, R. Deng, M. Teng, Q. Li, Y. Yang, X. Hu, Z. Zhang, G. Zhang, Microchim. Acta 185 (2018) 1.
[66] S.L. Clauson, J.M. Sylvia, T.A. Arcury, P. Summers, K.M. Spencer, Appl. Spectrosc. 69 (2015) 785.
[67] M.B. Mamián-López, R.J. Poppi, Anal. Bioanal. Chem. 405 (2013) 7671.
[68] Z. Guo, L. Chen, H. Lv, Z. Yu, B. Zhao, Anal. Methods 6 (2014) 1627.
[69] M. Li, H. Wu, Y. Wu, Y. Ying, Y. Wen, X. Guo, H. Yang, J. Raman Spectrosc. 48 (2017) 525.
[70] L. He, M. Lin, H. Li, N.J. Kim, J. Raman Spectrosc. 41 (2010) 739.
[71] K.Y. Hong, C.D.L. de Albuquerque, R.J. Poppi, A.G. Brolo, Anal. Chim. Acta 982 (2017) 148.
[72] F. Vajhadin, S. Ahadian, J. Travas-Sejdic, J. Lee, M. Mazloum-Ardakani, J. Salvador, G.E. Aninwene II, P. Bandaru, W. Sun, A. Khademhossieni, Biosens. Bioelectron. 151 (2020) 111984.
[73] M. Labib, E.H. Sargent, S.O. Kelley, Chem. Rev. 116 (2016) 9001.
[74] M. Majdinasab, A. Hayat, J.L. Marty, TrAC, Trends Anal. Chem. 107 (2018) 60.
[75] R. Zeng, Z. Luo, L. Zhang, D. Tang, Anal. Chem. 90 (2018) 12299.
[76] R. Zeng, Z. Luo, L. Su, L. Zhang, D. Tang, R. Niessner, D. Knopp, Anal. Chem. 91 (2019) 2447.
[77] R. Zeng, L. Zhang, Z. Luo, D. Tang, Anal. Chem. 91 (2019) 7835.
[78] L. Huang, Z. Yu, J. Chen, D. Tang, ACS Appl. Bio Mater. 3 (2020) 9156.
[79] E. Mousset, D.D. Dionysiou, Environ. Chem. Lett. 18 (2020) 1301.
[80] C. Chauhan, Mater. Today:. Proc. 37 (2021) 3231.
[81] R.R. Chillawar, K.K. Tadi, R.V. Motghare, J. Anal. Chem. 70 (2015) 399.
[82] R. Rajamanikandan, M. Ilanchelian, Anal. Methods 11 (2019) 97.
[83] S.S.J. Xavier, C. Karthikeyan, A.R. Kim, D.J. Yoo, Anal. Methods 6 (2014) 8165.
[84] T.S.H. Pham, P.J. Mahon, G. Lai, A. Yu, Electroanalysis 30 (2018) 2185.
[85] A.A. Gill, S. Singh, Z. Nate, C. Pawar, R. Chauhan, N.B. Thapliyal, R. Karpoormath, R. Patel, J. Pharm. Biomed. Anal. (2021) 114219.
[86] J.M. George, R.N. Priyanka, B. Mathew, Microchem. J. 155 (2020) 104686.
[87] X. He, W.G. Aker, M.-J. Huang, J.D. Watts, H.-M. Hwang, Curr. Top. Med. Chem. 15 (2015) 1887.
[88] H. Razmi, H. Shirdel, R. Mohammad-Rezaei, Micro Nano Lett. 12 (2017) 217.
[89] B. Rafiee, A.R. Fakhari, Biosens. Bioelectron. 46 (2013) 130.
[90] A.M. Santos, A. Wong, A.A. Almeida, O. Fatibello-Filho, Talanta 174 (2017) 610.
[91] X. Zhang, Y. Wei, Y. Ding, Anal. Chim. Acta 835 (2014) 29.
[92] B. Shen, X. Wen, G.V. Korshin, Environ. Sci. Processes Impacts 20 (2018) 943.
[93] R. Chauhan, A.A. Gill, Z. Nate, R. Karpoormath, J. Electroanal. Chem. 871 (2020) 114254.
[94] N.R. Jalal, T. Madrakian, A. Afkhami, M. Ghamsari, J. Electroanal. Chem. 833 (2019) 281.
[95] Y. Zhang, X. Cai, X. Lang, X. Qiao, X. Li, J. Chen, Environ. Pollut. 166 (2012) 48.
[96] J. Shan, R. Li, K. Yan, Y. Zhu, J. Zhang, Sens. Actuat., B 237 (2016) 75.
[97] X. Fang, X. Chen, Y. Liu, Q. Li, Z. Zeng, T. Maiyalagan, S. Mao, ACS Appl. Nano Mater. 2 (2019) 2367.
[98] K. Abnous, N.M. Danesh, M. Alibolandi, M. Ramezani, S.M. Taghdisi, A.S. Emrani, Sens. Actuat., B 240 (2017) 100.
[99] Z. Zhang, Q. Liu, M. Zhang, F. You, N. Hao, C. Ding, K. Wang, J. Hazard. Mater. 416 (2021) 125988.
[100] S.M.T. Heidarian, A.T. Sani, N.M. Danesh, M. Ramezani, M. Alibolandi, G. Gerayelou, K. Abnous, S.M. Taghdisi, Sens. Actuat., B 334 (2021) 129632.
[101] M. Mahmoudpour, H. Kholafazad-kordasht, J.E.N. Dolatabadi, M. Hasanzadeh, A.H. Rad, M. Torbati, Anal. Chim. Acta (2021) 338736.
[102] L. Bábelová, M.E. Sohová, A. Poturnayová, M. Buríková, J. Bizík, T. Hianik, Electroanalysis 30 (2018) 1487.
[103] Y. Gao, H. Qi, M. Shang, J. Zhang, J. Yan, W. Song, Biosens. Bioelectron. 146 (2019) 111741.
[104] Z.-J. He, T.-F. Kang, L.-P. Lu, S.-Y. Cheng, J. Electroanal. Chem. 860 (2020) 113870.
[105] A.L. Furst, M.B. Francis, Chem. Rev. 119 (2018) 700.
[106] Z. Qiu, D. Tang, J. Shu, G. Chen, D. Tang, Biosens. Bioelectron. 75 (2016) 108.
[107] M. Xu, Z. Gao, Q. Wei, G. Chen, D. Tang, Biosens. Bioelectron. 74 (2015) 1.
[108] L. Hou, X. Wu, G. Chen, H. Yang, M. Lu, D. Tang, Biosens. Bioelectron. 68 (2015) 487.
[109] L. Hou, Y. Tang, M. Xu, Z. Gao, D. Tang, Anal. Chem. 86 (2014) 8352.
[110] T. Bertok, L. Lorencova, E. Chocholova, E. Jane, A. Vikartovska, P. Kasak, J. Tkac, ChemElectroChem 6 (2019) 989.
[111] V.P. Gajdosova, L. Lorencova, A. Blsakova, P. Kasak, T. Bertok, J. Tkac, Curr. Opin. Electrochem. 28 (2021) 100717.
[112] X. Hu, K.Y. Goud, V.S. Kumar, G. Catanante, Z. Li, Z. Zhu, J.L. Marty, Sens. Actuat., B 268 (2018) 278.
[113] I. Ahmed, S.H. Jhung, Coord. Chem. Rev. 441 (2021) 213989.
[114] M. Wang, M. Hu, J. Liu, C. Guo, D. Peng, Q. Jia, L. He, Z. Zhang, M. Du, Biosens. Bioelectron. 132 (2019) 8.
[115] X. Liu, D. Huang, C. Lai, G. Zeng, L. Qin, H. Wang, H. Yi, B. Li, S. Liu, M. Zhang, Chem. Soc. Rev. 48 (2019) 5266.
[116] X. Yan, Y. Song, J. Liu, N. Zhou, C. Zhang, L. He, Z. Zhang, Z. Liu, Biosens. Bioelectron. 126 (2019) 734.
[117] Q.-Q. Zhu, W.-W. Zhang, H.-W. Zhang, R. Yuan, H. He, J. Mater. Chem. C 8 (2020) 16984.
[118] F. Giroud, K. Gorgy, C. Gondran, S. Cosnier, D.G. Pinacho, M.-P. Marco, F.J. Sánchez-Baeza, Anal. Chem. 81 (2009) 8405.
[119] M. El-Maghrabey, N. Kishikawa, S. Harada, K. Ohyama, N. Kuroda, Biosens. Bioelectron. 160 (2020) 112215.
[120] J. Yu, W. Tang, F. Wang, F. Zhang, Q. Wang, P. He, Sens. Actuat., B 311 (2020) 127857.
[121] Y. Yao, C. Jiang, J. Ping, Biosens. Bioelectron. 123 (2019) 178.
[122] V. Gaudin, Biosens. Bioelectron. 90 (2017) 363.
[123] J. Wang, Z. Liu, TrAC, Trends Anal. Chem. (2020) 116089.
[124] D. Long, M. Li, H. Wang, H. Wang, Y. Chai, R. Yuan, Biosens. Bioelectron. 142 (2019) 111579.
[125] C. Sui, T. Wang, Y. Zhou, H. Yin, X. Meng, S. Zhang, G.I. Waterhouse, Q. Xu, Y. Zhuge, S. Ai, Biosens. Bioelectron. 127 (2019) 38.
[126] J. Shu, Z. Qiu, Z. Lin, G. Cai, H. Yang, D. Tang, Anal. Chem. 88 (2016) 12539.
[127] B. Jin, Z. Jiao, Y. Bi, J. Mater. Chem. A 3 (2015) 19702.
[128] R. Tanwar, B. Kaur, U.K. Mandal, Appl. Catal. B 211 (2017) 305.
[129] P. Yan, L. Xu, D. Jiang, H. Li, J. Xia, Q. Zhang, M. Hua, H. Li, Electrochim. Acta 259 (2018) 873.
[130] M. Sun, Y. Zhu, K. Yan, J. Zhang, Biosens. Bioelectron. 145 (2019) 111712.
[131] S. Hu, Y. Yu, Y. Guan, Y. Li, B. Wang, M. Zhu, Chin. Chem. Lett. 31 (2020) 2839.
[132] Y. Zhang, Y. Teng, Y. Qin, Z. Ren, Z. Wang, Anal. Lett. 53 (2020) 660.
[133] Z. Li, H. Zhang, Q. Zha, C. Zhai, W. Li, L. Zeng, M. Zhu, Microchim. Acta 187 (2020) 1.
[134] L. Xu, H. Li, P. Yan, J. Xia, J. Qiu, Q. Xu, S. Zhang, H. Li, S. Yuan, J. Colloid Interface Sci. 483 (2016) 241.
[135] C. Yuan, Z. He, Q. Chen, X. Wang, C. Zhai, M. Zhu, Appl. Surf. Sci. 539 (2021) 148241.
[136] M. Li, H. Wang, X. Wang, Q. Lu, H. Li, Y. Zhang, S. Yao, Biosens. Bioelectron. 142 (2019) 111535.
[137] W. Wang, Q. Sang, M. Yang, J. Du, L. Yang, X. Jiang, X. Han, B. Zhao, Sci. Total Environ. 702 (2020) 134956.

[138] J.-H. Zhu, Y.-G. Feng, A.-J. Wang, L.-P. Mei, X. Luo, J.-J. Feng, Biosens. Bioelectron. 181 (2021) 113158.
[139] Z. Guo, K. Jiang, H. Jiang, H. Zhang, Q. Liu, T. You, J. Hazard. Mater. 424 (2022) 127498.
[140] K. Dashtian, S. Hajati, M. Ghaedi, Sens. Actuat. B 326 (2021) 128824.
[141] W. Zhuge, X. Li, S. Feng, Microchem. J. 155 (2020) 104726.
[142] H.-F. Tsai, Y.-C. Tsai, S. Yagur-Kroll, N. Palevsky, S. Belkin, J.-Y. Cheng, Lab Chip 15 (2015) 1472.
[143] H. Kholafazad-kordasht, M. Hasanzadeh, F. Seidi, TrAC, Trends Anal. Chem. (2021) 116455.
[144] A. Nakhlband, H. Kholafazad-Kordasht, M. Rahimi, A. Mokhtarzadeh, J. Soleymani, Microchem. J. 173 (2022) 107042.
[145] S. Chen, S. Brahma, J. Mackay, C. Cao, B. Aliakbarian, J. Food Sci. 85 (2020) 517.
[146] W.-C. Kao, S. Belkin, J.-Y. Cheng, Anal. Bioanal. Chem. 410 (2018) 1257.
[147] J. Liu, B. Wang, H. Huang, D. Jian, Y. Lu, Y. Shan, S. Wang, F. Liu, Food Chem. 335 (2021) 127596.
[148] M.H.B. Tafti, M.R. Ishaghi, P. Rajaei, Meat Sci. (2021) 108605.
[149] B. Fu, X. Zheng, H. Li, L. Ding, F. Wang, D.-Y. Guo, W. Yang, Q. Pan, Sens. Actuat., B 346 (2021) 130502.
[150] J. Hua, Y. Jiao, M. Wang, Y. Yang, Microchim. Acta 185 (2018) 1.
[151] C. Wu, R. Cheng, J. Wang, Y. Wang, X. Jing, R. Chen, L. Sun, Y. Yan, J. Sep. Sci. 41 (2018) 3782.
[152] Z. Li, Z. Cui, Y. Tang, X. Liu, X. Zhang, B. Liu, X. Wang, M.S. Draz, X. Gao, Microchim. Acta 186 (2019) 334.
[153] R. Bosma, J. Devasagayam, A. Singh, C.M. Collier, Sci. Rep. 10 (2020) 1.
[154] R. Gui, X. Bu, W. He, H. Jin, New J. Chem. 42 (2018) 16217.
[155] B. Liu, Y. Huang, Q. Shen, X. Zhu, Y. Hao, P. Qu, M. Xu, RSC Adv. 6 (2016) 100743.
[156] M.K. Pawar, K.C. Tayade, S.K. Sahoo, P.P. Mahulikar, A.S. Kuwar, B.L. Chaudhari, Biosens. Bioelectron. 81 (2016) 274.
[157] X. Yuan, W. Lv, B. Wang, C. Yan, Q. Ma, B. Zheng, J. Du, D. Xiao, Spectrochim. Acta Part A Mol. Biomol. Spectrosc. 253 (2021) 119599.
[158] T. Madrakian, S. Maleki, A. Afkhami, Sens. Actuat., B 243 (2017) 14.
[159] H. Tan, L. Zhang, C. Ma, Y. Song, F. Xu, S. Chen, L. Wang, ACS Appl. Mater. Interf. 5 (2013) 11791.
[160] B. Zhang, Y. Sun, K. Pang, X. Wang, Biosensing and nanomedicine Xi, Int. Soc. Opt. Photon. (2018) 107280N.
[161] J. He, G. Song, X. Wang, L. Zhou, J. Li, J. Alloys Compd. 893 (2022) 162226.
[162] Z. Tao, J. Du, Y. Cheng, Q. Li, Int. J. Electrochem. Sci. 13 (2018) 1413.
[163] S.M. Taghdisi Heidarian, A. Tavanaee Sani, N.M. Danesh, M. Ramezani, M. Alibolandi, G. Gerayelou, K. Abnous, S.M. Taghdisi, Sens. Actuat. B 334 (2021) 129632.